AN ABSTRACT OF THE THESIS OF

Jay Albert Dotter for the degree of Master of Science

in Geology presented on June 9, 1977

Title: PRAIRIE MOUNTAIN LAKES AREA, SE SKAGIT COUNTY, WASHINGTON: STRUCTURAL GEOLOGY, SEDIMENTARY PETROGRAPHY, AND MAGNETICS

Abstract approved: Redacted for privacy

Dr. Robert D. Lawrence

The thesis area is divided into three regions by tectonic boundaries (the Shuksan thrust and the Straight Creek fault). The rock units in these regions are the gneiss and pre-Eocene intrusives east of the Straight Creek fault, the Shuksan Schist west of the Straight Creek fault and north of the Shuksan thrust, and the mélange unit west of the Straight Creek fault and south of the Shuksan thrust. Along the Straight Creek fault are found tectonic slivers of the Swauk Formation.

A mélange is a mappable body of deformed rock made up of intact blocks of exotic or native materials in a pervasively sheared, commonly pelitic matrix. The blocks may range up to several miles in length. In the mélange unit of the thesis area the sandstones, conglomerates, and limestones of the sedimentary strata (Chilliwack Group?) are the native blocks, the siltstones are the pervasively sheared pelitic matrix, and the meta-igneous rocks are the exotic blocks. The sedimentary strata were deposited as a deepsea fan

building eastward off of an island arc into an intra-arc basin. The meta-igneous rocks (including meta-andesites, meta-basalts, meta-diorites, and meta-quartz diorites) are fragments of the oceanic crust of this intra-arc basin and are a partial source for the sedimentary strata. The mélange may have been produced, in a manner similar to the formation of the Franciscan Formation, along a west-facing subduction zone.

The Shuksan Schist (composed of greenschists, blueschists, and phyllites often interbanded) is part of a paired metamorphic belt that was formed deep within a subduction zone. When subduction ceased this unit was rapidly carried to the surface (less than 1 m.y.) and thrust into its present position. The pre-Eocene intrusives (including a hornblende diorite, mixed granites, and migmatite) are probably the result of diapiric upwellings on the continent side of the subduction zone. The gneiss (Skagit Gneiss?) is a quartz, actinolite gneiss that is probably metamorphosed continental crust. The rocks of the three regions were widely separated during their deposition and metamorphism and owe their present juxtaposition to plate convergence.

The magnetic study of the Sauk Prairie indicates that the average thickness of the glacial debris over the bedrock is 150m ± 25m. The magnetic modeling shows that the observed anomalies can be the result of: 1. relief of a basement of uniform magnetic susceptability; 2. blocks of varying magnetic susceptabilities at a uniform depth, or 3. a combination of these. The magnetic modeling also indicates where the maxima and minima of basement relief must occur and where the blocks of greater magnetic susceptability are located within the blocks of lesser magnetic susceptability, along with the relative sizes of the blocks.

The magnetic study of the eastern section shows that the location of the Straight Creek fault cannot be determined by one magnetic signature, but can be determined by a variety of magnetic signatures. These magnetic signatures might possibly be used to determine rock types juxtaposed across the Straight Creek fault in covered areas.

Prairie Mountain Lakes Area, SE Skagit County, Washington: Structural Geology, Sedimentary Petrography, and Magnetics

by

Jay Albert Dotter

A THESIS

submitted to

Oregon State University

in partial fulfillment of the requirements for the degree of

Master of Science

Completed 9 June 1977

Commencement June 1978

APPROVED:

Redacted for privacy

Associate Professor of Geology
in charge of major

Redacted for privacy

Chairman of Department of Geology

Redacted for privacy

Dean of Graduate School

Date thesis is presented June 9, 1977

Typed by Lyndalu Sikes for Jay Albert Dotter

ACKNOWLEDGEMENT

I wish to express my appreciation to my wife Judy who proof read much of this manuscript and gave me moral support. To my daughter Kara for the moral support she gave me and her repeated offers to color my geologic map. To Dr. Robert D. Lawrence, my major professor, who suggested this study, gave me much valuable aid and critically read this manuscript. To Dr. Richard W. Couch for his valuable help on the magnetics section and for critically reading this manuscript. To Dr. Harold E. Enlows and Dr. Frederick W. Obermiller for critically reading this manuscript. To Dr. Ansel Johnson (PSU) and Portland State University Geology Department for the use of their Geometrics proton precession magnetometer. To OSU Computer Science Center for the unfunded research grant that enabled me to use the CDC-3300 computer.

TABLE OF CONTENTS

TABLE OF CONTENTS (Continued)

LIST OF TABLES

LIST OF ILLUSTRATIONS

LIST OF ILLUSTRATIONS (Continued)

PRAIRIE MOUNTAIN LAKES AREA, SE SKAGIT COUNTY, WASHINGTON: STRUCTURAL GEOLOGY, SEDIMENTARY PETROGRAPHY, AND MAGNETICS

INTRODUCTION

Purposes of This Study

The purposes of this study were to: 1. construct a detailed geologic map of the area at a scale of 1:20,000; 2. study in detail the sedimentary petrography of the Sedimentary unit with emphasis on petrographic analysis to discover their depositional environment and the type of their source rocks; 3. interpret the structural geology and sequence of faulting; 4. determine the subsurface geology of the Sauk Prairie from total field magnetic data using Peters' (1947) half-slope method and computer modeling; 5. locate more accurately the trace of the Straight Creek fault from total field magnetic data and outcrop information; and 6. compare sandstone from the Swauk Formation, Nooksack Group, and Chilliwack Group using Dickinson's method (1976) to determine their depositional environment with respect to a converging plate boundary.

Equipment and Materials

The base maps used were the Darrington 7.5 minute Quadrangle, Washington, and the Prairie Mountain 7.5 minute Quadrangle, Washington. Aerial photographs on a 1:20,000 scale and NASA high altitude aerial photographs on a 1:60,000 scale were used in the field and in the laboratory to complement the base maps.

A Brunton compass was used to obtain attitudes on planar features in the field. A Geometrics proton precession magnetometer, borrowed from Portland State University, was used in the magnetic survey. A CDC 3300 computer and a programmable calculator were used to reduce the magnetic data obtained in the survey.

Thesis Area

The thesis area lies on the western flank of the Northern Cascades in Skagit County, Washington (Figure 1). It comprises most of the northern half of the Prairie Mountain quadrangle (1:24,000) and lies across the Suiattle River, east of the Sauk River. This area is approximately 52 square kilometers, and is situated entirely in T33N, R10E, and R11E. Since the section numbers in the thesis area do not overlap, all locations referred to by the township and range system hereafter will use only the section numbers.

The Suiattle River flows down a large glacial U-shaped valley that runs diagonally through the thesis area from the southeast to the northwest (see Figure 1). Its elevation is from 219m in the southeast to 165m in the northwest. The highest point in the thesis area (1670m) is in the northeast corner, only 2.9km from the Suiattle River, making a maximum relief of 1505m. The highest point in the southwestern section is 1267m. The majority of the thesis area is composed of steep slopes, all of which are heavily wooded. Many of these slopes contain old clear cuts, which are extremely difficult to navigate. Over all but the highest peak in the area is a covering of till and/or colluvium, which totally obscures bedrock in most places. Fortunately, logging roads cross much of the area, producing reasonable access and the majority of outcrops. Thus, there are enough outcrops in much of the area to

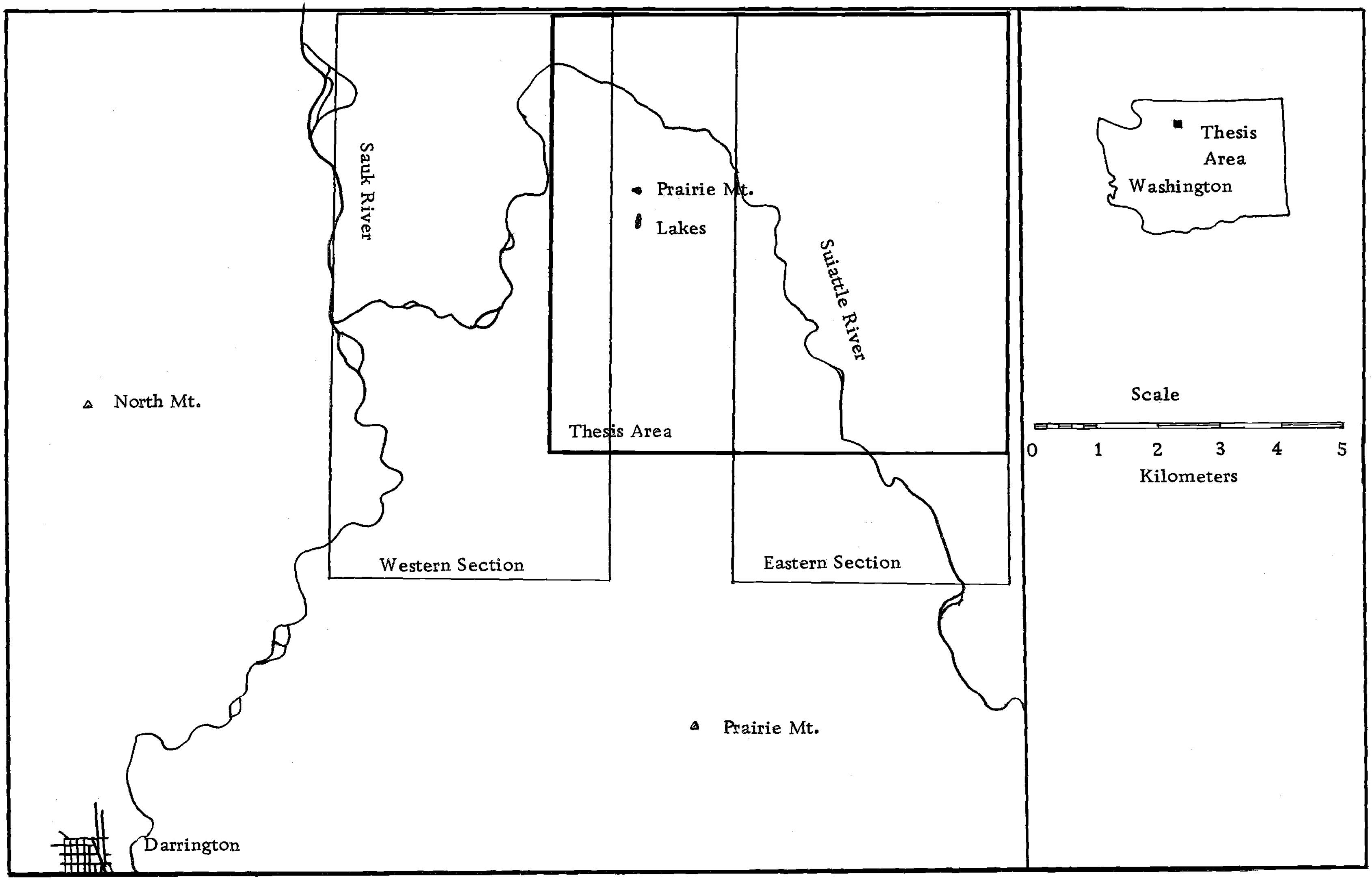

Figure 1. Location map of thesis area and magnetic survey sections.

construct a reasonably accurate geologic map (see Plate 1).

Previous Work in the Area

Since 1949 Misch (1966) and students working under him have reconnaissance mapped much of the North Cascades. Misch has mapped the region north of the Cascade River. Bryant (1955) made a reconnaissance study of the Snowking area, north of the Suiattle River. Vance (1957) did the geology of the Sauk River area south of the Suiattle River. The thesis area incorporates the northernmost section of Vance's area and the southernmost section of Bryant's. Lawrence (unpublished manuscript, 1972) has mapped much of the area surrounding the thesis area. Franklin (1975) mapped the area directly to the south of the thesis area and Milnes (1977) mapped the area directly to the north. Others who have worked in the area are: Tabor (1961); Tabor and Crowder (1969); Crowder, Tabor, and Ford (1966); Danner (1966); Grant (1969); Johnson and Couch (1970); and Mattinson (1970, 1972).

Regional Geology

The Straight Creek fault of Eocene age (Vance, 1957) runs north-south through the eastern half of the thesis area and is traceable from the Ellensburg, Washington area north to the Chilliwack batholith, which cuts the Straight Creek fault and was intruded into it from Late Eocene to Miocene. McTaggart (1970) believes the Straight Creek fault is an extension of the Frazer River fault zone of Canada. The Straight Creek fault is a major structural boundary in the western North Cascades. It separates Misch's (1966) Skagit Metamorphic Suite (Pb/U metamorphic ages ranging from 60 to

1,650 m.y. (Mattinson, 1972)) and the Pre-Eocene intrusives on the east, from the Shuksan Schist (K/Ar metamorphic ages ranging from 218 to 259 m.y. (Misch, 1966)) and the mélange unit (containing rocks of Ordovician to Late Permian age (Misch, 1966; Danner, 1966; and Vance, 1957, 1974)) on the west.

The member of the Skagit Metamorphic Suite present in and around the thesis area is correlated with the Skagit gneiss of Misch (1966), which is of the barrovian facies. This unit was intruded by the pre-Eocene intrusive unit during the Late Mesozioc to Early Tertiary (Huntting, et al., 1961).

The Shuksan Schist which includes greenschists, blueschists, and graphitic phyllite in the thesis area is of the lower blueschist facies (Brown, 1974) and is traceable from the Clu Elum region in the south-central Cascades northward to Mt. Shuksan (Franklin, 1975). Rocks of the Shuksan Schist have been thrust southwestward to westward over the mélange unit in an imbricate manner. The basal thrust of the Shuksan thrust system (partially in the thesis area) separates the Shuksan Schist to the northeast from the mélange unit to the southwest. The mélange unit is composed of blocks of sedimentary rocks (possibly of the Chilliwack Group (Vance, 1957)) and blocks of meta-igneous rocks in a pervasively sheared pelitic matrix of the sedimentary rocks. The sedimentary rocks are lithic wackes, siltstones, conglomerates, and limestones. The meta-igneous rocks include meta-diorites, meta-andesites, and meta-basalts (among others) and are believed to be fragments of intra-arc oceanic crust (Lawrence, personal communication, 1977).

The youngest rocks of the region, other than Quaternary deposits, are of the Swauk Formation, which is a fluvial sequence of arkosic wackes, siltstones, and conglomerates. The Swauk Formation occurs mainly to the south and southeast of the central core of the Northern Cascades. In and around the thesis area, the

Swauk strata are found as tectonic slivers caught up in the Straight Creek fault zone.

Quaternary deposits include abundant glacial debris, alluvium, and alluvial fans. The glacial debris is the result of extensive Pleistocene glaciation (Mackin and Cary, 1965) that covered all but the highest peaks in the area and carved all the major valleys. Glacial phenomena, such as moraines, kettles, kame terraces, and striated pavement are abundant in the region and attest to the severe degree of glaciation.

UNIT DESCRIPTIONS AND PETROGRAPHY

Introduction

For convenience in description, the rock units exposed in the thesis area are divided into three tectonically bounded regions. These are 1. those east of the Straight Creek fault, 2. those in the Straight Creek fault, and 3. those west of the Straight Creek fault. The rock units east of the Straight Creek fault are gneisses (Skagit gneiss?) and pre-Eocene intrusives (hornblende diorite, mixed granites, and migmatite). The rock unit incorporated in the Straight Creek fault is the Swauk Formation. The rock units west of the Straight Creek fault are 1. the mélange unit containing sedimentary rocks (Chilliwack Group?) which include conglomerates, sandstones, siltstones, and limestones and meta-igneous rocks which include meta-diorites, meta-andesites, and meta-basalts, 2. the Shuksan Schist which is subdivided into a greenschist unit and a phyllite unit.

Procedural Methods

During the 1976 field season, the investigator mapped the study area and collected 222 rock samples. These rock samples were slabbed and polished, then grouped into the major units the investigator found in the study area. A selective sample was taken of each group for thin section analysis. A total of 88 thin sections were studied by the investigator. Fifty-nine of these thin sections were from rocks collected by the investigator, while the remainder were from the collection of Dr. Robert D. Lawrence. The distribution by rock unit of the 78 thin sections from the thesis area studied by the investigator is presented in Table 1.

A standard Leitz binocular petrographic microscope was used with a white light source. Rock classifications used were the IUGS classification for plutonic rocks (Geotimes, 1973); Gilbert's classification of sandstones (Williams, et al., 1954); Folk's classification of carbonate rocks (Folk, 1962); and metamorphic rocks as classified by Spry (1969). Volume percentages of minerals for all sandstones with authigenic matrix no greater than 50% were determined by point counts. The number of points counted depended upon the volume percent of matrix. Where the volume percent of matrix was less than 20%, a 500 to 600 point count was considered sufficient. Where the volume percent of matrix exceeded 20%, a 650 to 750 point count was made. In the remainder of the thin sections, the volume percents were determined by visual estimation.

Table 1. Thin sections per unit.

Rock Unit	Number of Thin Sections Major Units	Subunits
Rocks east of the Straight Creek fault		
Pre-Eocene intrusives	10	
Hornblende diorite		6
Mixed granite and migmatite		4
Gneiss	3	3
Rocks in the Straight Creek fault		
Swauk Formation	8	8
Rocks west of the Straight Creek fault		
Shuksan Schist	15	
Greenschist unit		14
Phyllite unit		1
Mélange unit	52	
Meta-igneous unit		23
Sedimentary rocks		
sandstone		16
marbles		2
Mylonites		11
TOTALS	87	87

ROCK UNITS EAST OF THE STRAIGHT CREEK FAULT ZONE

Introduction

For this study the rocks east of the Straight Creek fault were divided into three units: gneiss, hornblende diorite, and other pre-Eocene intrusives. The gneiss is found in the northeast corner of the map and along the crest of Huckleberry Mountain. The hornblende diorite occurs in the northeast corner of the map and intrudes the gneiss. The other pre-Eocene intrusives are found in Huckleberry Mountain and the ridge north of it. Another small crop of these pre-Eocene intrusives is found in the SE1/4 of the SW1/4 of section 8.

Gneiss

In the study area, the gneiss crops out in roadcuts and stream channels. Of the rock types found in this area, the gneiss appears to be the least resistant to weathering. Generally it is highly sheared, which may partially account for this erodibility. This shearing is probably related to movement of the Straight Creek fault and/or post-metamorphic intrusive activity.

In handspecimen, the gneiss is a medium to coarsely crystalline rock which has a strong gneissic foliation. These rocks have undergone intense folding. Small scale macroscopic folds are abundant. Both similar and parallel folds are present and their attitudes range from upright to overturned.

Petrographic study of the gneiss shows a banded, granoblastic, polygonal texture with veins of coarsely crystalline quartz and prophyroblasts of garnet and actinolite. The major minerals and their volume percents (based on a 350 point count of a typical sample) are: quartz, 41%; actinolite, 37%; albite, 10%; and biotite, 9%. The accessory minerals present are garnet and magnetite (see Appendix C, Table C-5). The percentage of garnet appears to be quite variable (ranging from trace proportions to approximately 80%), while the relative abundances of the other minerals appear to be fairly constant. The gneiss appears to have a moderate metamorphic rank and is probably of the upper greenschist facies.

Hornblende Diorite

In the thesis area, a unit of hornblende diorite crops out as cliffs, in roadcuts, and in stream channels. It is a very resistant unit and forms the highest point in the study area. It continues beyond the study area to the north and east.

This unit displays much variability. Macroscopic inspection reveals a phaneritic, holocrystalline rock, which is finely to coarsely crystalline (hornblende crystals up to 4cm long) and exhibits a granular to porphyritic texture. Hornblende is present in all outcrops, but its volume percent decreases gradually from 100% at its first exposure at the 850m level on the slope east of Grade Creek to 15% at the 1350m level (see Plate I). In the roadcut at the switchback in the SW1/4 of the NW1/4 of section 5, this unit is rhythmically layered (see Figure 2). The layers have sharp upper and lower contacts and are composed of hornblende-rich bases grading upward to plagioclase-rich tops. The layers range in thickness from 1cm to 20cm and appear to be of cumulate origin. A cumulate origin would explain the hornblendite base, the increase in plagioclase upward with concomitant decrease of hornblende, and

Figure 2. Rhythmic layering in the hornblende diorite unit.

the layering. The hornblende diorite unit appears to be a layered igneous intrusion, similar to the Skaergaard or the Palisade Sill (Wager and Brown, 1962).

Petrographic study of two samples from this unit indicates that the essential minerals are hornblende and plagioclase (andesine and labradorite). Other minerals that occasionally reach essential proportions are interleaved biotite and muscovite, orthoclase, quartz, and garnet. Pyrite and zircon occur as minor minerals.

Other Pre-Eocene Intrusive Rocks

These intrusive units are not differentiated on the geologic map of the thesis area (Plate I). Their contacts are sharp, but too little exposure is available to define their interrelationships beyond the observation that they are very complex. The various rock types included in this unit were classified after visual inspection of handspecimens. In general, they are phaneritic, holocrystalline rocks that are medium to coarsely crystalline. The rock types identified are a migmatite (Figure 3), a granite porphyry, an equigranular biotite granite, and an equigranular muscovite granite.

Petrographic analysis was run on a typical sample of the biotite granite. The volume percent of each of its minerals is based on a 300 point count. The essential minerals are: albite, 37%; quartz, 31%; orthoclase, 18%; and biotite, 14%. The accessory minerals, which make up less than 5% of the rock, are magnetite, apatite, zircon, sphene, and garnet (see Appendix C, Table 5).

Unit Relationships East of the Straight Creek Fault Zone

The contact relationships between the rock units east of the Straight Creek fault are intrusive, but the relationships between

Figure 3. Boulder of migmatite.

units can be divided into three kinds: 1. a narrow zone (50m wide) of complex intrusive interrelationships that occurs from 475m to 525m elevation, 2. Skagit gneiss occurs predominately as roof pendents, and 3. occurrance of migmatites that appear to have an intrusive origin.

East of the Straight Creek fault there are only three outcrops that occur in the thesis area between 475m and 525m. Each of these shows a very complex, intrusive interrelationship between the three types of granites present and the Skagit gneiss. The interrelationship is in the form of small veins (3-60m wide) of the granites injected into the Skagit gneiss, with the remaining Skagit gneiss in the form of narrow lenses (10-30m). These veins are oriented approximately perpendicular to the north-south trend of this zone. This zone of complex, intrusive interrelationships appears to form the western fringe of the pre-Eocene intrusive activity.

In the higher elevations of the thesis area, the outcrops of gneiss are surrounded by igneous rock and appear to be remnants of roof pendents. In the north section at lower elevations, the Skagit Gneiss appears to surround the hornblende diorite intrusion and delineate the boundary of the intrusion.

Not many outcrops of migmatite are found in the thesis area. However, to the east on Huckleberry Mountain and the ridge north of Tenas Creek migmatites are the predominant rock type exposed. From the relationships observed between the various intrusive rocks in the thesis area, this investigator believes that the migmatite unit may be the result of multiple intrusions into the hornblende diorite. These multiple intrusions may have broken the hornblende diorite into blocks and surrounded the blocks with granitic veins. Thus this would be the varity of migmatite called an agmatite.

Correlation and Age

The gneisses east of the Straight Creek fault have been correlated by Misch (1966) with the Skagit Gneiss, and Mattinson (1972) obtained Pb/U metamorphic ages for the Skagit Gneiss of 415 m.y. and 60 to 90 m.y. The pre-Eocene intrusives were first mapped by Bryant (1955) in this area. He assigned a Mesozoic age to this unit, and since this unit is cut by the Eocene Straight Creek fault it must be pre-Eocene.

ROCK UNITS WEST OF THE STRAIGHT CREEK FAULT ZONE

Introduction

The Shuksan Schist unit includes a greenschist unit and a phyllite unit. The Shuksan Schist occurs west of the Straight Creek fault and north of the basal Shuksan thrust fault. The basal thrust of the Shuksan thrust system trends northwest-southeast and is found just west of the Suiattle River in the thesis area, from the southern end of the map (see Plate I) northward to the NW1/4 of section 14. At this location the basal thrust is offset by a right-lateral tear fault and presumably runs northward under the alluvium to the NW1/4 of section 11, where it is again offset by a right-lateral tear fault. The basal thrust is then found to trend almost east-west in the SE1/4 of section 3 on out of the thesis area. There is a large band of the phyllite unit in section 2 which, in this locality, occurs approximately 0.75 km behind the basal Shuksan thrust. This band of phyllite is offset by the tear fault (in section 11, 12, and 13) and presumably exists under the alluvium of the Suiattle River.

Shuksan Schist

Greenschist Unit

The Greenschist is very resistant to erosion and crops out in the thesis area as prominant cliffs, as ledges, in roadcuts, and in stream channels, often as waterfalls.

The Greenschist is a fine to medium crystalline rock which displays a variable development of schistosity. The range is from a very poor schistosity which is discernable only in thin section to a very strong schistosity that is easily evident in hand specimens. This reflects a varying chlorite and amphibole content in the rocks. This unit is finely banded (less than 1cm thick). The banding is recognized in the field as alternate bands of light green and of dark green to blue. The bands are generally linear, except within a few meters of a thrust fault where they become highly folded on a small scale (2 to 20cm wavelengths and 1 to 5 cm amplitudes). The amount of blue amphibole present varies from none to approximately 8%. This variation appears to represent a trend in the thesis area of greenschist grading upward stratigraphically to a banded blue-greenschist and gradually into a blueschist. This trend, which is from a low metamorphic grade to a higher metamorphic grade, is in general perpendicular to the local trend of the Shuksan thrust fault.

Thin sections of 14 Shuksan Greenschist samples were studied. The major minerals present in the true greenschists were actinolite, epidote, quartz, and chlorite. The major minerals present in the blueschists were glaucophane, crossite, epidote, actinolite, and quartz. The difference between the two schists is the amount of blue amphibole present. A complete gradation between the blue-schists and the greenschists was found in the field. This gradation was also evident in thin section analysis. The gradational rocks usually had bands rich in glaucophane and crossite, alternating with bands rich in actinolite, epidote, and chlorite. Pyrite and sericite are often present as accessory minerals, while calcite is occasionally present.

Phyllite Unit

Outcrops of the phyllite unit in the thesis area are found in roadcuts and in streams. It is not resistant to erosion and erodes rapidly. It is easily recognized in the field due to its black color and its many white layers of quartz and albite. These layers are generally highly folded with wavelengths ranging from .5 cm to a few centimeters and amplitudes from .2 cm to 2 cm. Many folds are overturned and isolated fold noses are often found. The minerals observed in handspecimens are graphite, quartz, and albite. No thin sections were analyzed. This is a low grade metamorphic rock. A detailed analysis of the Darrington Phyllite which is believed to be a correlative of this unit is underway by David A. Jenne (OSU thesis in progress).

Correlation and Age

The Shuksan Schist can be followed from its type locality at Mt. Shuksan through the thesis area and on to the south. Kulp dated the greenschists, as reported by Misch (1966), using K/Ar. He obtained metamorphic ages of 218 m.y. and 259 m.y. for the greenschists and Misch (1966) reports whole rock ages of Middle Cretaceous for the Darrington Phyllite. The phyllite unit of the Shuksan Schist was correlated with the Darrington Phyllite by Misch (1966) and Vance (1957).

The investigator and others (Lawrence, personal communication, 1977; Milnes, 1977) believe that the phyllite unit and the greenschist unit are codepositional and that the Middle Cretaceous age for the Darrington Phyllite represents the most recent degassing event, this being the movement of the Shuksan thrust. The Shuksan Schist appears to be a low to medium grade metamorphic rock that grades from the lower greenschist facies to the lower blueschist facies (Brown, 1974) and was derived from mafic volcanic rocks (Misch, 1966). The greenschist unit with its greenschists and blueschists is similar to the paired metamorphic belts found along subduction zones (Ernst, 1972; Miyashiro, 1972; and Oxburgh and Turcotte, 1971).

Unit Relationships in the Shuksan Schist

Field mapping and photo interpretation indicate that the Shuksan Greenschist in the thesis area consists of a sequence of imbricate thrust sheets separated by layers of contorted phyllite. The phyllite unit appears to have acted as a lubricant between thrust sheets. The investigator noticed in the field that the degree of contortion in the phyllite unit was greatest at the contacts with the schist and decreased rapidly as the distance from the contact increased. The thrust relationship will be further discussed in a later section of this thesis. There are several locations in the thesis area where the Shuksan Schist and the phyllite unit are found as thin, alternating bands (see Figure 4). Large sections of this rock type are exposed in Pet Rock Creek from the 300 m elevation to the 550 m elevation, and in the SW1/4 of the SW1/4 of section 30 (Plate I). Another occurrence is along the streams in the SW1/4 of section 2. The latter two outcrops are probably part of the same thrust sheet, while the occurrence in section 30 appears to be from a separate sheet. A thin banding, similar to this in scale but involving alternate layers of greenschist and blueschist, was observed in the rocks in the upper part of the ridge west of Grade Creek. Between these two units of intermixed rocks was found the

Figure 4. Alternating thin bands of greenschist and phyllite.

banded greenschist. The scale of banding in the banded greenschist is similar to the scale of banding observed in the intermixed rocks. These bands apparently are due to compositional layering inherent in the parent rock with the average metamorphic grade increasing to the northeast.

Mélange Unit

Introduction

A mélange has been defined as a mappable body of deformed rock made up of intact blocks of exotic or native materials in a pervasively sheared, commonly pelitic matrix. The blocks may range up to several miles long (Hsü, 1968). In the mélange unit of the thesis area, sandstones, conglomerates, and meta-igneous rocks acted competently, while siltstones acted incompetently under the shear stress that produced the mélange. The sandstone and conglomerate are the native blocks, the meta-igneous rocks are the exotic blocks, and the siltstones are the pervasively sheared pelitic matrix (Figure 5). To the southwest in Franklin's area (Franklin, 1975) exotic blocks of blueschist occur in addition to the meta-igneous blocks. Many of the sedimentary and meta-igneous blocks are separately mappable, as can be seen in Plate I.

The mélange unit is found southwest of the basal thrust of the Shuksan thrust system. Two large meta-igneous blocks occur in the southern section separated by small pods of the sedimentary rocks and a narrow zone of undifferentiated mélange. Another large zone of undifferentiated mélange occurs further to the west. A large block of sedimentary rock is found to the north of the two large meta-igneous blocks and in the northern most area of the mélange is a small meta-igneous block. Several small blocks of sedimentary

Figure 5. Chilliwack sandstone bed in sheared siltstone.

strata, meta-igneous, and undifferentiated mélange are scattered throughout the mélange unit. The areas of undifferentiated mélange are where the blocks of sedimentary strata and meta-igneous rocks are too small to map separately and occur haphazardly in the sheared pelitic matrix. The sedimentary strata of the mélange have been tentatively correlated with the Chilliwack group (Vance, 1957).

Meta-igneous Rocks of the Mélange

The meta-igneous rocks are the most resistant to erosion of those in the mélange unit. The majority of the high points, cliffs, and ridges in this section of the thesis area are underlain by these rocks.

The meta-igneous rocks include both intrusive and extrusive rocks, as well as tectonic breccias and mylonites formed from these rocks. In outcrop and handspecimen these rocks are very difficult to identify. Rocks belonging to the meta-igneous group are easily recognized in thin section, but it was often difficult to classify the igneous rock type. This difficulty was caused by the severe degree of alteration in the plagioclases. Since the majority of the feldspars displayed abundant exsolution features and extreme seritization, determination of the plagioclase type was very difficult and often dubious. Only where reliable plagioclase determinations could be achieved was a meta-igneous rock further classified. The igneous rock types thus determined from the thin section analysis are a porphyritic basalt, a porphyritic diorite, a quartz diorite, and a porphyritic andesite.

Of the andesites studied, three were vesicular, hemicrystalline with phenocrysts of oligoclase and a ground mass of devitrifying glass and plagioclase microlites. One of these samples also had phenocrysts of augite. Another sample was holocrystalline and had phenocrysts of andesine, hornblende, orthoclase and an opaque mineral in an aphanitic groundmass of plagioclase. All samples showed extensive seritization and chloritization. One sample contained celadonite, while another contained palagonite.

Of the diorites studied, the samples had phenocrysts of andesine and augite in a phaneritic groundmass of the same minerals that displayed a diabasic texture. Abundant chlorite and kaolinite were present as alteration products.

The quartz diorite studied was a holocrystalline, medium-grained, phaneritic, equigranular rock. The major minerals were quartz, andesine, and orthoclase. The accessory minerals included epidote and opaques. The alteration products present were calcite, chlorite, and sericite.

The basalt studied was a porphyritic rock with an aphanitic groundmass. The phenocrysts present were augite, an orthopyroxene, an amphibole (possibly cummingtonite), and altered plagioclases.

Many samples of the meta-igneous mylonite were studied. These all showed a fluxion structure and usually displayed aligned fine-grained micas. Prophyroclasts ranged in size from .5 mm to 6 mm. The porphyroclasts observed were quartz, plagioclase, orthoclase, augite, opaques, and fragments of meta-igneous rocks. A more detailed discussion of the meta-igneous rocks in the adjacent area is given by Franklin (1975).

Discussion

Franklin (1975) described a unit he informally designated the "All Creek Volcanics" and considered to be of Tertiary age. He believed that the All Creek Volcanic unit was composed of a series of interrelated andesites, tuffs, and tuff breccias which filled the lower Suiattle valley and lay unconformably upon the Chilliwack Formation (sedimentary portion of the mélange unit herein). I followed a continuous outcrop of this unit northward from Franklin's thesis area into the present area of study. From my work, I believe that this "All Creek Volcanic" unit is actually a large meta-igneous block of the mélange. The limits of this block can be determined very easily by airphoto interpretation and compares very favorably with field evidence. My conclusion that the "All Creek Volcanics" unit is part of the mélange is based on petrographic evidence. I observed andesites and tuff breccias, as Franklin did (1975), in addition I found basalts and porphyritic diorites in this block. The porphyritic diorite from this block is very similar to a sample of the porphyritic diorite obtained 1.5 km northwest from the furthest outcrop in this block. Both of these samples are porphyritic with a phaneritic groundmass that displays a diabasic texture. Furthermore, they have the same mineralogies and are altered to the same degree. These are the only samples like this I found in the thesis area. Also there is a vesicular andesite with a large percentage of celadonite. Pebbles of a vesicular andesite with a large percentage of celadonite occur in the conglomerate at the top of the "All Creek Volcanic" block and in one of the very coarse grained sandstones. A rock similar to this andesite is also found in the meta-igneous block to the west. Because the "All Creek Volcanic" block contains at least two different rocks that are also found in the meta-igneous block to the west it is concluded that they are the same unit. Furthermore, because the sedimentary rocks of the mélange unit contain grains of the "All Creek Volcanics" meta-igneous block, this block must be at least partially the source for the sedimentary rocks and therefore older than the sedimentary rock. Additionally, the conglomerate found at the top of the "All Creek Volcanics" meta-igneous block is in depositional contact with the underlying meta-igneous rocks and is believed to be the basal conglomerate of the sedimentary unit of the mélange.

Correlation and Age

The meta-igneous rocks have been correlated by Misch (1966) with the Turtleback Formation of the San Juan Islands and the Yellow Astor Complex of northwest Washington. Rocks of the Yellow Astor Complex have been radiometricly dated by Mattinson (1972) at 1,650 m.y. and 450 m.y. Misch (1966) views these rocks as fragments of continental crust emplaced by westward thrusting from the crystalline core of the Cascades to the east. Vance (1974) argued that these are fragments of a thinned continental crust that was marginal to an ocean basin formed by continental rifting. Franklin (1975), based on the intimate association of the meta-igneous rocks with the paired metamorphic belt (Shuksan Schist) and the lack of radiometric correlation between the meta-igneous rocks and the existing crystalline core, argued that the meta-igneous rocks are fragments of either oceanic crust or island arc crust that were moved from their original position in the west eastward to their present position due to subduction processes. I believe that the meta-igneous rocks are crustal fragments of an intra-arc basin and owe their present position to subduction processes. These rocks are of an assemblage (diorites, quartz diorites, andesites, and basalts) that would be expected to form the oceanic crust of an intra-arc basin (Dickinson, 1972). The meta-igneous rocks are older than the sedimentary rocks of the mélange and were a partial source for them. This conclusion is based on the contact in section 25 where the basal conglomerate of the sedimentary unit is in depositional contact with the underlying meta-igneous block and from petrographic evidence that shows grains of the meta-igneous rocks in the coarser sedimentary strata (to be discussed in detail later). As will be shown in a later section, the probable depositional site of the sedimentary unit was a deepsea fan building off of an island arc. The depositional association of the sedimentary strata and the underlying meta-igneous rocks implies an intra-arc depositional site for these units that was immediately behind the arc (Karig, 1971, 1972).

Clastic Sedimentary Rocks of the Mélange

Sedimentary rocks of the mélange unit display a very low resistance to erosion. As such, they generally form the lower areas of the thesis area. The sedimentary rocks crop out in roadcuts, in stream channels, and less often along ridges. The few good outcrops that are found are sandstones. The siltstones have acted incompetently and in most outcrops they are highly sheared and conform to the boundaries of the sandstone blocks.

There are only a few good sandstone outcrops in the thesis area. The best of these is situated in a roadcut in the NE1/4 of the NE1/4 of the SW1/4 of section 14. In this outcrop, there are several sandstone beds which range in thickness from .5 m to 2 m. The bedding contacts are sharp, generally regular, and continuous over the 15 m length of the crop. These sandstones range in average grain size from very fine grained to very coarse grained, although there is only one very coarse grained sandstone exposed here. It is a channel deposit with a concave, upward, cut-and-fill type lower contact with the underlying fine grained sandstone. In several other outcrops where very fine grained sandstones and sandy siltstones occurred, thin, parallel laminations were observed. No other sedimentary structures were observed in mélange sedimentary rocks in the thesis area. Rhythmically graded bedding was observed by the investigator in an outcrop of related strata situated approximately

10 km south of the thesis area.

Sedimentary structures seen in thin sections of the sedimentary strata are confined to the fine to very fine grained sandstones and the sandy siltstones. The medium and coarser grained sandstones appear to be structureless. All the thin sections of the fine grained sandstones and siltstones show thin parallel laminations. Several of the thin sections displayed fine cross-laminations and two thin sections show soft sediment deformation in the form of slump folds and contorted bedding.

The textures seen in thin section appear to vary with grain size. The very coarse to medium grained sandstones tend to be poorly sorted, have rounded to subangular grains, and usually contain less than 20% matrix. The fine and very fine grained sandstones tend to be poorly to moderately sorted, have angular to subangular grains, and contain greater than 30% matrix.

Of the 16 thin sections of the sedimentary strata of the mélange studied, only four were suitable for point counts. The rest were greatly sheared or authignic matrix was greater than 50%, making them inappropriate for statistical study. Two of the point counts were carried out on the same thin section. This thin section was cut across the contact between a very coarse grained sandstone and a fine grained sandstone, each side being point counted separately. The other thin sections studied appear to be very similar to those point counted in modal composition. Therefore, those point counted are considered to be a representative sample. The results of the point counts are presented in Appendix C, Table 1. As can be seen, the major minerals are generally the same for each sample, but the volume percent shows a large variation. The volume percent of polycrystalline quartz ranges from 0% to 23%, while the volume percent of quartz varies from 14% to 29%. In these four samples, an inverse relationship of the volume percent is found between quartz and polycrystalline quartz. This is why the total adjusted volume percent of quartz plus polycrystalline quartz is fairly constant (the adjusted volume percent is recalculated with all matrix excluded). The volcanic lithics, including chert-like material which in these samples is believed to be devitrified volcanic glass, show a marked size dependence. With increasing grain size, the volcanic lithic content increases. Such a size dependence has been well documented in the literature (Pettijohn et al., 1972). This size dependence is also quite evident in the ternary plot of these samples (Figure 6), in which the four samples form a straight line. The remaining major minerals, the feldspars, occur in relatively constant proportions with the exception of the very coarse sandstone. Here, there is only a trace of plagioclase and 1% of orthoclase. This sample also shows a decrease in quartz and polycrystalline quartz and contains over 64% lithic fragments. The deficiency of feldspars may be explained by multiple source areas for these rocks.

These samples, when plotted on Gilbert's ternary classification diagrams (Williams et al., 1954), are lithic wackes (Figure 6). The wacke diagram was used since all the samples of the sedimentary strata of the mélange from the thesis area contain more than 10% matrix. The majority of the matrix is believed to be of an authogenic origin. This conclusion is based on the destruction of grain boundaries by the growth of matrix minerals and on the large volume percentages of matrix.

Limestones

Four outcrops of marble and one outcrop of limestone were found in the thesis area. The marbles were medium to coarse

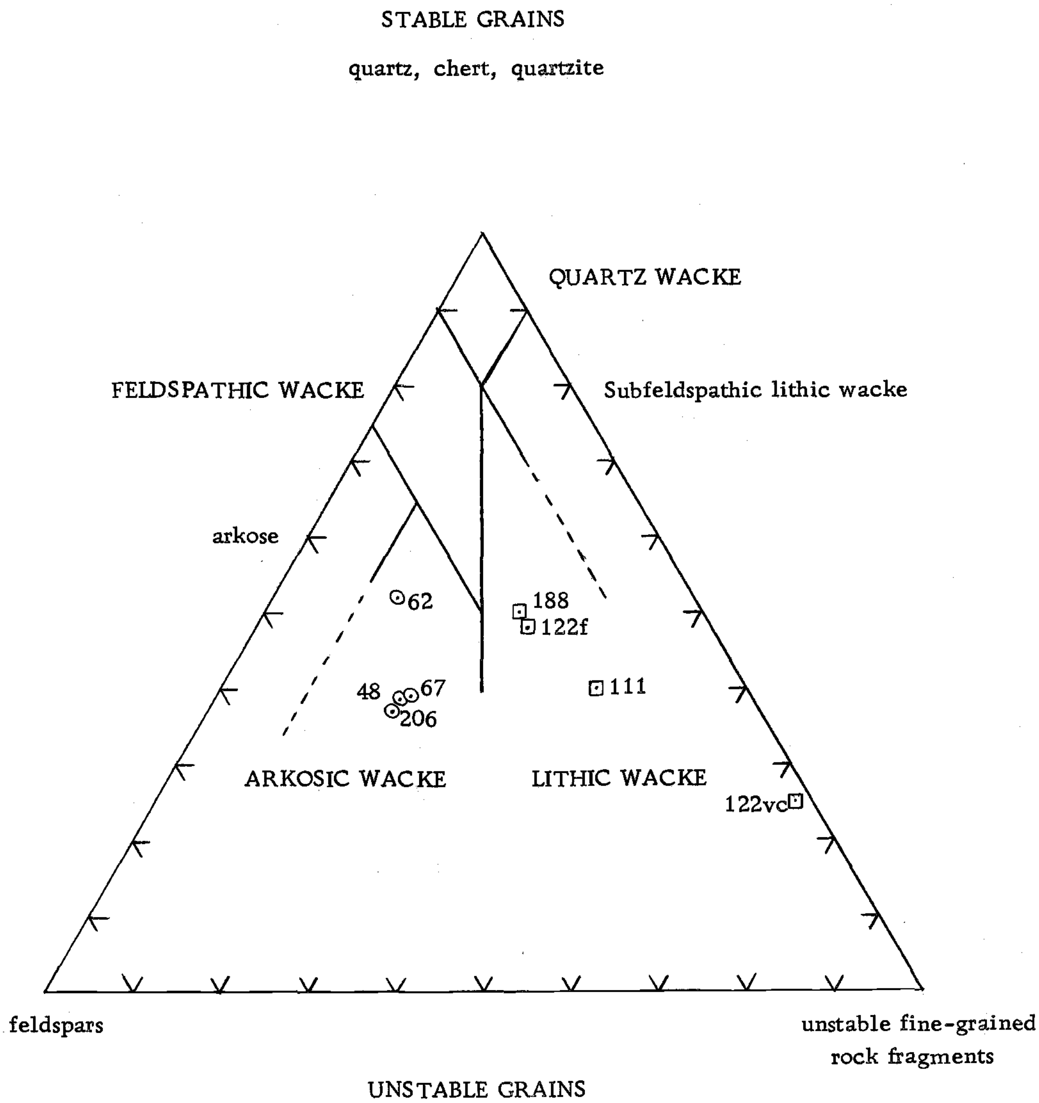

Chilliwack sandstones from thesis area

Swauk sandstones

Figure 6. Classification of Chilliwack and Swauk sandstones.

grained with an elongate, equigranular, polygonal texture. The four outcrops are very small and appear to be tectonic lenses.

The limestone outcrop is situated on a small knob just north of the road in the SW1/4 of the SE1/4 of the NW1/4 of section 14. This rock is dark gray, appears massive in handspecimen, and is easily mistaken for a meta-igneous rock. The sample is divided in half by a folded vein of calcite with quartz along the center of the vein. The lower-half (stratigraphically) of this rock is a mottled micrite. The mottling is believed due to burrowing. The burrows are pinched out as they approach the nose of the fold. The folding is believed to be a form of soft sediment deformation, probably caused by the drag produced by the flow depositing the overlying intramicrite. The overlying intramicrite is composed predominantly of intraclasts of mottled micrite, presumably rip ups of the underlying mottled micrite. The intraclasts range in size from 1 to 15 mm. They are elongate and well rounded. There appear to be fossils in this sample, several possible foraminifera (Bostwick, personal communication, 1977), and another type of fossil that is circular. The circular fossils are approximately .25 mm in diameter. They have been generally replaced by pyrite, but several are of calcite and some are of both calcite and quartz. The calcite appears to be replacing the quartz. This rock appears to have been deposited in a deep marine environment.

Correlation and Age

The sedimentary strata of the mélange unit has been tentatively correlated by Vance (1957) with the Chilliwack Group described by Daly (1912). The Chilliwack strata have been dated from fossils found in the small limestone units as Devonian to Permian (Danner, 1966; Misch, 1966). Data from Danner (1966), dating the limestones of the Chilliwack, shows that they occur in age belts with the oldest limestones of the unit in the northeast and the youngest limestones to the southwest. This suggests that the Chilliwack strata associated with the limestones have this same trend, and that the ages of the Chilliwack strata can be related directly to the closest limestone units. On this assumption, the Chilliwack strata of the thesis area are of Pennsylvanian age, based on the dating by Danner (1966) of large crinoid stems found in a limestone body in the Conn Creek area, south of the thesis area in the Whitechuck quadrangle.

Depositional Environment

It is doubtful that a unique determination can be made of the depositional environment for the Chilliwack strata from information obtained in the thesis area. This is because the Chilliwack strata is contained in the mélange unit. The age of the Chilliwack Group ranges from Devonian to Permian (Danner, 1966; Misch, 1966). The blocks of Chilliwack strata may represent only one time period or all the time periods of deposition. During the possible 170 million years of deposition, the depositional environment may have changed drastically and repeatedly. This could easily cause juxtaposition of Chilliwack blocks from varied depositional environments.

If all the Chilliwack blocks in the thesis area are assumed to have been deposited in the same depositional environment, then a possible depositional environment may be determined. This interpretation is supported by distinct age bands of the Chilliwack strata based on fossil dates of the limestones of the unit (Danner, 1966).

The sedimentary structures found in the Chilliwack strata of the thesis area and their method of formation are: 1. very thinly laminated fine sandstones and siltstones, which require either weak constant currents or periodical overbank flooding on a small scale; 2. very thinly cross-laminated beds, that require slightly higher current velocities than those that form sandstones and siltstones such as those described above; and 3. soft sediment deformation features, which are caused by slumping on a slight slope.

An examination of the textures found in the Chilliwack strata of the thesis area suggests some depositional mechanisms. The poor sorting of the sandstones requires fairly rapid deposition with little or no reworking. The high degree of angularity requires short transport distances. The variable average grain size of the sandstones requires currents of varying competency. The channel containing the very coarse sandstone requires a competent, erosive current. The abundance of volcanic lithics requires a volcanic source and a short transport distance. The limestone, discussed previously, requires a deep marine depositional environment. A depositional environment in which these features could be found is a deepsea fan building off of an island arc into an intra-arc basin or onto the arc trench gap. The very finely laminated and cross-laminated fine sandstones and siltstones would represent the intra-channel areas of the fan. The laminations are the result of minor overbank flooding from the channels. The channels would allow a current competent enough to carry larger grains outacross the fan. These coarser grains would tend to be deposited in the channels. Poor sorting would be expected of the sands deposited in or near the channels. The slope required for the soft sediment deformation observed in thin section would be provided for by the fan. The limestone could also be an intrachannel deposit. This would explain the presence of silt for the formation of micrite. The deepsea fan model envisioned is that of Normark (1973), and the sedimentary structures, textures, and associations expected in a deepsea fan are from Nelson and Kulm (1973).

Dickinson (1972) states that volcanic wackes are predominantly derived from island arcs. He further states that the oceanic crust derived in an intra-arc basin would be of an amphibolitic character when metamorphosed and would be made up largely of basalts and andesites with small associated plutons of gabbro or diorite. The meta-igneous rocks are largely meta-andesites and meta-diorites. The rocks found in the thesis area conform well to the rock types Dickinson believes would be found in an intra-arc basin. The available data supports the proposed model, but more data from a much larger area is needed before a model such as this could be proved.

Discussion

In a sample of one of the very coarse grained sandstones from the thesis area, a somewhat unique volcanic lithic fragment was found. It was a highly vesicular volcanic glass that had been altered to celadonite. Rocks similar to this grain are found in the meta-igneous rocks and in rocks of what was once thought to be the All Creek Volcanics. It is thus possible that at least some of the source rocks were of the meta-igneous unit, and that these rocks must predate the Chilliwack sandstone that contains them.

ROCK UNIT FOUND IN THE STRAIGHT CREEK FAULT ZONE

Swauk Formation

Outcrops of the Swauk strata are found on the lower valley sides along Grade Creek and the lower nose of the ridge north of Huckleberry Mountain. These outcrops are found in roadcuts into the valley sides.

In outcrop the Swauk Formation was found to be composed of interbedded mudstones, siltstones, and sandstones. The coarsest grained sample of Swauk strata found in the thesis area was a pebbly sandstone. Sedimentary structures observed in outcrop include thin laminations and cross-laminations, bedding and cross-bedding, cut-and-fill contacts, channels, flame structures, load casts, parting lineations (with aligned carbonaceous plant fragments), and some normally graded beds. The mudstones and siltstones are highly fractured near the tectonic contacts. Mud rip ups and carbonaceous plant fragments were found near the bases of several beds.

Modal analyses of Swauk sandstone were determined from four samples by point counting (see Appendix C, Table 2). The major minerals are: quartz, 22-26%; plagioclase, 11-22%; orthoclase, 11-15%; and lithic fragments, 9-17%. The minor minerals generally present are biotite and muscovite. Many other minerals occur in trace amounts in one or two of the thin sections. The matrix content varies from 12-23%. These four samples plot as arkosic wackes (see Figure 6).

The Swauk Formation is generally believed to be a fluviatile sequence of Paleocene age (Foster, 1960). The data obtained in the thesis area tends to support this depositional environment. It was apparently deposited on a low erosional surface cut across most of the Cascade Range at the end of Cretaceous time (Foster, 1960; Mackin and Cary, 1965).

Correlation and Age

The tectonic slivers of sedimentary rocks found in the Straight Creek fault zone were correlated by Vance (1957) with the Swauk Formation. These rocks are of Late Cretaceous to Paleocene in age based on fossil leaves contained within them (Vance, 1957; Foster, 1960).

COMPARISON OF CHILLIWACK, SWAUK, AND NOOKSACK SANDSTONES

Introduction

The purpose of this comparison was to see if the distribution of petrographic types in the clastic Chilliwack strata is similar to the geographic distribution of ages found in the limestones of the Chilliwack Group. An additional purpose was to determine if the clastics of the Chilliwack Group are significantly different from other major clastic sedimentary units of the area (Swauk Formation and Nooksack Group). Chilliwack sandstones used to check this hypothesis were collected near dated limestones. Because of their metamorphic overprint some of the samples collected as sandstones turned out to be dike rocks so the sampling of Chilliwack sandstones was incomplete.

Modal analyses were completed on four thin sections of Chilliwack sandstones from the thesis area; on three thin sections of Chilliwack sandstones from Jackman Creek, Washington; on four thin sections of Swauk sandstones from the thesis area; and on three thin sections of Nooksack sandstones from north of Mt. Baker. The results of the modal analysis are presented in Appendix C, as are brief rock descriptions of the Nooksack and Chilliwack sandstones from outside the thesis area. Rock descriptions of the Swauk and Chilliwack sandstones from the thesis area are presented above.

Method of Comparison

The samples of Chilliwack, Swauk, and Nooksack sandstones were compared using a method developed by Dickinson (1976). This method is used to determine the depositional environment of a sandstone with respect to a converging plate boundary. Dickinson's method involves the use of refined ternary diagrams for the classification of sandstones. Instead of using one ternary diagram with quartz, feldspar, and lithic end members, three ternary diagrams are used. Their end members are: 1. monocrystalline quartz (Qm), feldspar (F), and lithics plus polycrystalline quartz (L + Qp); 2. monocrystalline quartz, plagioclase (P), and potassic feldspar (K); 3. polycrystalline quartz (Qp), volcanic lithics (Lv), and sedimentary lithics (Ls). For interpretation of depositional environments using this method, it is assumed that: 1. the polycrystalline quartz present was derived from chert deposited in a deep marine environment; 2. the volume of volcanic and sedimentary lithics will increase as an arc is approached; 3. as erosion of a volcanic arc continues, the erosional products will be, first, volcanic lithics, then feldspars and monocrystalline quartz from the plutonic root of the arc.

Comparison

When plotted on Gilbert's classification system (Williams, et al., 1954), the sandstones analyzed in this study show distinct groupings (see Figure 7). The Chilliwack samples from Jackman Creek are lithic wackes with very little quartz (less than 12%) and a moderate amount of feldspar (14-22%). The Chilliwack samples from the thesis area are also lithic wackes, but they contain much more quartz (14-29%) and less feldspar (1-13%) than the Chilliwack from Jackman Creek. The Swauk sandstones are arkosic wackes, and the Nooksack sandstones range from lithic wackes to arkosic wackes.

When these samples are plotted on the Qm - F - L + Qp ternary diagram of Dickinson, the three samples of Chilliwack from Jackman

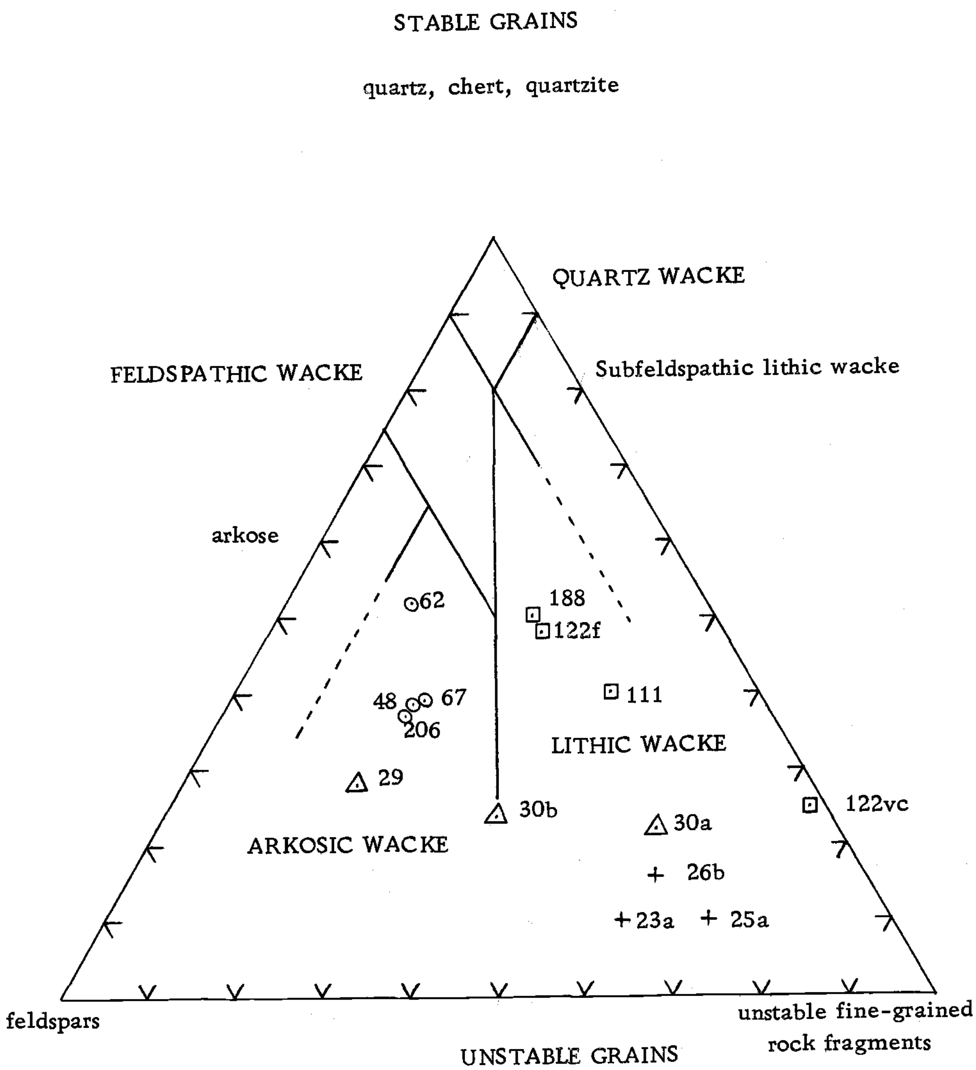

Chilliwack sandstones from thesis area

Swauk sandstones

Nooksack sandstones

Chilliwack sandstone from Jackman Creek

Figure 7. Classification of chilliwack, Swauk, and Nooksack sandstones.

Creek and the two coarser samples of Chilliwack from the thesis area plot near the L + Qp corner of the diagram (see Figure 8). This suggests that the depositional environment of the Chilliwack was near a young volcanic arc being actively eroded. These five samples are coarse to very coarse grained sandstone. The other two Chilliwack samples (122f and 188) are fine grained sandstones, which precludes the possibility of a large volume of lithics. The Nooksack samples display a large variability, which is suggestive of continued erosion of a volcanic arc, thereby making available a larger volume of plutonic minerals. The Swauk samples plot near the Qm - F (plutonic) side of the diagram. This is reasonable since the Swauk is a fluviatile sequence developed late in the history of the area after erosion had exposed considerable plutonic material.

On the Qp - Lv - Ls diagram, the Chilliwack from Jackman Creek plots in the Lv corner. There is very little polycrystalline quartz present in these samples. The samples of Chilliwack from the thesis area all plot on the Qp - Lv side of the diagram, yet there is a large range in the volume of polycrystalline quartz. This variability could be caused by varied depositional environments with sample 111 representing the most oceanic sediment. This seems doubtful based on the thin section analyses, as the polycrystalline quartz observed in these samples was either meta-quartzite or devitrified volcanic glass. The presence of volcanic glass indicates a less mafic source for samples 188 and 111 than for sample 122. On the Qm - F - L + Qp diagram, samples 122vc and 122f are at opposite ends of the variability, while on the Qp - Lv - Ls diagram they plot within 8% of one another. This is caused by the difference in grain size and suggests that 122f and 122vc share a common source. The Nooksack samples, when plotted on a Qp - Lv - Ls diagram, show a large variability. These samples plot along the

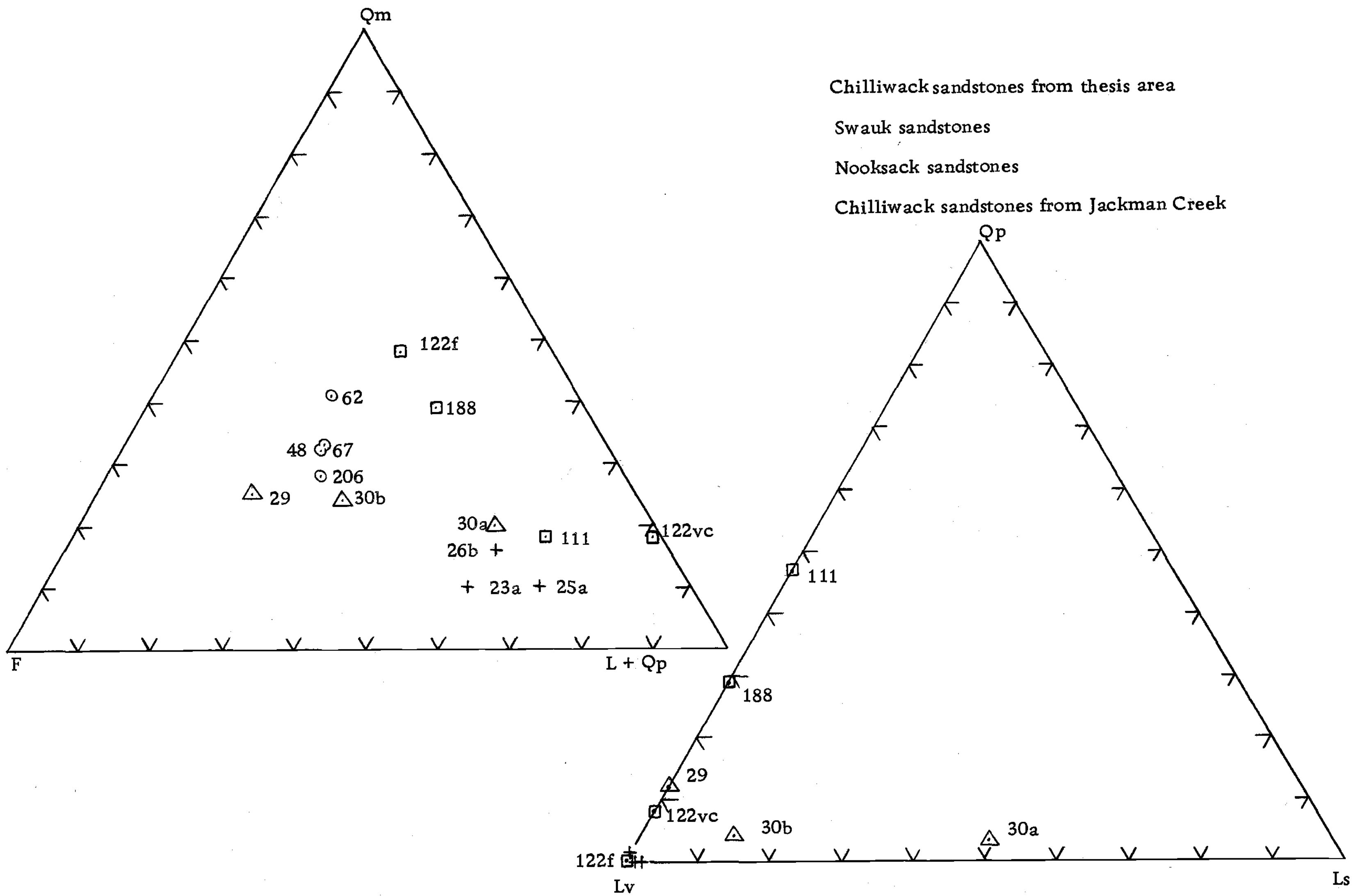

Figure 8. Qm - F - L + Qp and Qp - Lv - Ls diagrams.

Lv - Ls side of the diagram and suggest an arc environment. The Swauk samples were not plotted on the Qp - Lv - Ls diagram because they have an extremely low volume of volcanic lithics, sedimentary lithics and polycrystalline quartz.

These samples were collected from units of widely separated ages and from locations that are far apart. The Chilliwack samples from the thesis area are of probable Pennsylvannian age. The Chilliwack samples from Jackman Creek are of Devonian age and occur approximately 32 km to the northwest of the thesis area. The Nooksack samples are of Early Cretaceous age and occur approximately 65 km to the northwest of the thesis area. The Swauk samples are from the thesis area and are of Paleocene age.

In general, too small a sample was used to obtain more than mere suggestive trends. The samples do not plot neatly as arcs or oceanic depositional sites. This ambiguity may be the result of an intra-arc basin depositional site where true oceanic depths were not attained.

STRUCTURE

Introduction

Structure in this area is dominated by faulting. There are two sets of thrust faults, tear faults associated with the thrusts, a right lateral strike slip fault (Straight Creek Fault), and a northeast-southwest trending vertical fault with the northwest side relatively up.

Thrusts in the Mélange

There are two thrust faults that can clearly be distinguished in the mélange unit. Others may be present but could not be separated from the general mélange shearing. Those seen generally have a north-south trend and an eastward dip. They are recognized on the ground and on aerial photographs of the area. The eastern thrust fault separates an essentially volcanic member of the meta-igneous unit and its overlying basal Chilliwack conglomerate from a zone of undifferentiated mélange. Because the surface trace of the fault tends to move eastward with decreasing elevation, its dip must be to the east. The western fault has meta-igneous rocks on both sides of the fault plane, except at the northern end, where it has Chilliwack strata on both sides. The evidence for this fault dipping to the east is that it runs along the bases of a series of cliffs with a maximum height of 120 m. In order for these cliffs to face westward as they do, the thrust fault at their bases must dip into them, or eastward. Furthermore, in sections 23 and 24, the fault runs along a series of small north-south trending valleys that occur on the west side of Prairie Mountain. The west sides of these valleys (downhill side) are low ridges that are similar to cuestas. The uphill or eastern side of these ridges dip at approximately 30° to the east, while the downhill side dips at approximately 50° to the west. The eastern side of these ridges is the dip slope of the fault. Thrusting occurred on these faults near the end of the mélange cycle or after the mélange was formed, as evidenced by the thrusts cutting both Chilliwack strata and meta-igneous rocks. These thrust faults ceased activity prior to thrusting of the Shuksan thrust system (Middle Cretaceous, Misch, 1966).

Shuksan Thrust System

The Shuksan thrust system is a series of imbricate thrust faults that generally have a northwest-southeast trend and dip to the northeast. There are at least six thrust faults and two tear faults associated with this system in the thesis area, including the basal thrust (see Plate I). They are truncated on the east by the Straight Creek Fault and offset on the west by tear faults. These thrust faults are recognized in the field by the presence of narrow zones (3-15 m) of the phyllite unit and a rapid increase in small scale (2-10 cm amplitude) folding near the thrust faults. Furthermore, the outcrops of the greenschist unit in the thesis area west of the Suiattle River form what appear to be two cuesta-like structures, one behind the other. The two cuesta-like structures have near vertical cliffs on the southwest side and gently dipping slopes (20-30°) parallel to foliations and probably parallel to the thrust faults on their northeastern side. In aerial photographs the thrust faults generally appear as prominent lineations. Heavy forest and alluvial cover forces these faults to be based on incomplete data, but the map pattern shown must be similar to the actual pattern.

Evidence for a northeastward dip is: 1. the cuesta-like structures with their shallow dip-slope to the northeast, 2. foliations in the greenschist generally dip to the northeast, and 3. the thrust contacts are found to swing eastward with decreasing elevations.

The thrust fault model envisioned here is a series of concave upward thrusts with steep dips ($45-65^{o}$) at their forward end. These dips decrease rapidly with depth so that a near horizontal attitude is attained at a shallow depth. The thrust faults behind the basal thrust of the Shuksan system converge rapidly (within a few kilometers) with the basal thrust zone at an approximate depth of 200 m $\pm$ 150 m below sea level. Strong support for this model is found in the presence of a small pod of Chilliwack strata just west of the center of section 18 (see Plate I). This pod of Chilliwack strata is situated along a thrust fault of the Shuksan thrust system and lies 3 km from the next closest outcrop of Chilliwack strata. This exposure of Chilliwack strata strongly suggests that the mélange unit extends back at least this far under the Shuksan Schist, and that the mélange unit at this location cannot be very far (approximately 550 m $\pm$ 150 m) below the surface (see Plate I, cross section C-B).

The tear faults were located by outcrop data, aerial photograph interpretation, and geometric considerations. In the thesis area they have offset the basal thrust of the Shuksan system a total of 1.8 km. These tear faults show that the thrust faults of the mélange unit occurred prior to the thrust faults of the Shuksan system because the tear faults are limited to the Shuksan Schist and do not continue into the mélange unit. Further evidence of prior thrusting of the thrust faults in the melange unit is found in sections 14 and 15, where a northeast-southwest trending fault cuts the thrust in the mélange but does not appear to cut the overlying Shuksan Schist. Mapping of these faults is subject to minor variations in interpretation due to the lack of exposure under the Suiattle River alluvium, but must basically have a pattern similar to that shown.

Straight Creek Fault

The Straight Creek fault is a right-lateral, transverse fault (Misch, 1966) that can be followed on high altitude aerial photographs from Ellensburg, Washington, north to the Chilliwack Batholith in northern Washington. McTaggart (1970) believes that the Straight Creek fault is an extension of the Frazer River fault zone.

In the thesis area the Straight Creek fault zone has a maximum width of 1 km. This zone is a series of anastomising, near vertical faults which enclose tectonic slivers of Swauk strata that have been rafted into place by the Straight Creek fault (see Plate I). This fault juxtaposes rocks of the Shuksan Schist on the west with rocks of the Skagit Gneiss and the pre-Eocene intrusive units on the east. Misch (1966) and Vance (1957) have dated movement on the fault as Eocene. Misch (1977) suggests some 120 miles of right-lateral displacement on the basis of matching metamorphic units.

Table 2. Sequence of formation of structures.

Major Structure	Approximate Time of Formation
1. Mélange	Post-Pennsylvannian to pre-Middle Cretaceous
2. Thrusts in the mélange	Post-mélange to pre-Middle Cretaceous
3. Northeast-southwest trending fault in the mélange	Post-thrusting in the mélange to pre-Middle Cretaceous
4. Shuksan Thrust system and associated tear faults	Middle Cretaceous
5. Straight Creek fault	Eocene

Degree and Sequence of Metamorphism

The rocks of the thesis area have undergone a long and varied metamorphic history. Again the structural barriers (Shuksan thrust and Straight Creek fault) separate areas with quite different metamorphic histories. The rocks in each of the three tectonic areas show different degrees of metamorphism. The Skagit Gneiss east of the Straight Creek fault attains the highest metamorphic grade of these rocks. In the thesis area the Skagit Gneiss just reaches the upper greenschist facies, but elsewhere it achieves the amphibolite facies (Misch, 1966). Mattinson (1972) reports metamorphic ages of 415 m.y., 90 m.y., and 60 m.y.

The Shuksan Schist, west of the Straight Creek fault and north of the basal Shuksan thrust, ranges from the lower greenschist facies to lower blueschist facies (Vance, 1974). Misch (1966) reports metamorphic ages for this unit of 259 m.y. and 218 m.y.

The mélange unit, west of the Straight Creek fault and south of the basal Shuksan thrust, is composed (in the thesis area) of blocks of two units. These units are the Chilliwack strata and the meta-igneous rocks. The Chilliwack strata in the thesis area is of Pennsylvannian age, and displays a light metamorphic overprint. It is debatable whether they can truthfully be considered to be metamorphosed. Their alteration has produced a large component of authigenic matrix. The meta-igneous rocks, as dated by Vance (1974), are Late Ordovician to Middle Devonian. Their metamorphic grade is slightly higher than that of the Chilliwack strata. In the meta-igneous rocks, the plagioclases display abundant exsolution features where a more sodic plagioclase is replacing a more calcic plagioclase. In many instances the exsolution has gone to completion, and crystals of albite are found in what was originally an andesite or basalt.

Because the meta-igneous rocks show a higher degree of metamorphism than the Chilliwack strata, with which they are intimately associated, they must have undergone one metamorphism prior to the formation of the mélange. Furthermore, since the Chilliwack was deposited on the meta-igneous rocks and the Chilliwack displays a much lower metamorphic grade, the initial metamorphism of the meta-igneous rocks in the thesis area must predate the deposition of the Chilliwack. Therefore, the initial metamorphism occurred before the Pennsylvannian and probably after the Middle Devonian. This time period predates the oldest known metamorphic age for the Shuksan Schist. Since the metamorphic grade of the Shuksan Schist is higher than that of the meta-igneous rocks, and the metamorphic age of the meta-igneous rocks is older than that for the Shuksan Schist, these two units must have been widely separated originally. Because the Shuksan Schist is presently to the east of the mélange unit and the two units were initially widely separated, either the Shuksan Schist originated far to the east of its present position (there is no evidence of this unit east of the Straight Creek fault) or the mélange unit was originally much further to the west. The latter possibility is the more likely one.

When comparing the Skagit Gneiss with the meta-igneous rocks, the same relationships are found as with the Shuksan Schist and the meta-igneous rocks. It is reasonable to assume that the same line of reasoning holds true, and the units of the mélange were initially deposited much farther away from the Skagit Gneiss than they now occur. Presumably, the mélange unit was initially deposited much further to the west.

A second episode of metamorphism effected the meta-igneous rocks. This was a light metamorphic overprint that is recognized in the Chilliwack strata. This episode occurred after or during the mélange formation and probably prior to movement of the Shuksan thrust. The most probable relative time for this episode of metamorphism was during the formation of the mélange.

Another feature that should be mentioned is the small scale folding of the bands in the Shuksan Schist (discussed above). Generally the banding of the Shuksan Schist is planar, except near the thrust faults, where they are highly folded. The intensity of folding increases rapidly near the thrusts. Presumably this folding of the banding is the result of stresses set up by movement of the Shuksan Schist along these thrust faults and indicates that thrusting occurred after the metamorphism of the Shuksan Schist. Also, it is doubtful that any metamorphism occurred after thrusting, otherwise this small scale folding of the banding would have been destroyed.

Table 4. Sequence of metamorphism.

Metamorphic Episode and/or Unit	Approximate Time of Metamorphism
1. Initial metamorphism of the meta-igneous rocks and the oldest known metamorphism of the Skagit Gneiss (probably concurrent but widely separated)	Late Ordovician to Middle Devonian for the meta-igneous rocks and 450 m.y. for the Skagit Gneiss.
2. Metamorphism of the Shuksan Schist	259 and 218 m.y.
3. Metamorphism of the mélange unit (light metamorphic overpring)	Post-Pennsylvannian to pre-Middle Cretaceous
4. Second episode of Skagit Gneiss metamorphism.	90 m.y.
5. Third episode of Skagit Gneiss metamorphism	60 m.y.

GEOLOGIC HISTORY

The meta-igneous rocks are the oldest rocks in the area; they are of Late Ordovician to Middle Devonian age (Vance, 1974). Vance believes the deposition of these rocks occurred on a thinned continental crust marginal to an ocean basin formed by continental rifting. The investigator and others (Lawrence, 1977; Franklin, 1975) view the meta-igneous rocks as fragments of oceanic crust formed in an intra-arc basin. The meta-igneous rocks were broken into blocks, some of the blocks were lifted above sea level, and then the basal conglomerate of the Chilliwack Group, which lies in depositional contact on the meta-igneous rocks, was deposited. Deposition of the Chilliwack Group began in Middle to Late Devonian and continued into Permian time (Danner, 1966; and Misch, 1966). It was deposited into an intra-arc basin as a deepsea fan building off an island arc. After deposition, the Chilliwack was broken up and mixed with blocks of the meta-igneous rocks to form the mélange unit. The break up of these rocks to form the mélange unit was probably an on-going process related to basin closure, similar to the formation of the Francisian Melange (Hsü, 1971).

During the Late Permian to the Early Triassic (Misch, 1966), the mélange unit was being further deformed by the thrusts found in the mélange unit. These thrusts are a series of north-south trending imbricate thrusts dipping to the east. At the same time, the Shuksan Schist was forming along a northeast-facing subduction zone on the eastern margin of the intra-arc basin. At the end of this period of subduction (Early Triassic), the Shuksan Schist was uplifted. Possibly the initial Shuksan thrust formed at this time and was the agent that uplifted the Shuksan Schist. For the period from Early Triassic to Middle Cretaceous, there is no evidence recognized presently in the rock record from which to interpret what happened geologically. Possibly there was another period of rifting, producing another intra-arc basin which then closed. Subduction occurred on the eastern margin west of the previous site. Near the Middle Cretaceous, subduction ceased and movement was renewed along the Shuksan thrust zone (Misch, 1966). The final movement along the Shuksan thrust zone was probably a result of the final stages of basin closure.

While the meta-igneous rocks were forming in the intra-arc basin, the Skagit Gneiss was forming to the east as part of the continental crust. This area appears to have been relatively inactive tectonically until the Mesozic to Paleocene intrusions of the pre-Eocene intrusives. After the intrusions were emplaced, the Northern Cascades were tectonicly quiet and underwent erosion, which formed a low erosional surface by the end of the Cretaceous that covered much of the Cascade Range (Mackin and Cary, 1965). The Paleocene Swauk Formation was deposited by streams and in lakes on this low erosional surface. During the Eocene right-lateral movement occurred along the Straight Creek fault, and tectonic slivers of Swauk strata were inducted into the fault zone and rafted to their present positions.

During the middle Tertiary and the Late Tertiary, volcanism was common in the central crystalline core of the Cascades and uplift occurred. In the Pliestocene, severe glaciation occurred which covered most of the Cascades with glacial debris and carved the major valleys.

MAGNETICS

Magnetic Survey

Survey Area

A magnetic survey was undertaken to attempt to determine a more precise location for the Straight Creek fault and also the sub-surface geology and/or structure of the Sauk Prairie area. For the purposes of this discussion, the two areas surveyed are designated the eastern section and the western section (Figures 9 and 10). The western section is directly west of the study area and covers part of the Sauk Prairie. The Sauk Prairie is a glacial outwash plain with bedrock covered by stratified outwash and till. Because glacial debris covers the Sauk Prairie, only magnetic data was obtained on the bedrock geology in this study.

Survey Procedure

The magnetic survey was conducted from 29 July 1977 to 3 August 1977, with a Geometrics total field proton precession magnetometer. The magnetometer has two units: the counter, which is carried on one's chest, and the sensor, which is carried on an eight foot aluminum staff.

The base maps used were the Darrington 7.5 minute Quadrangle, Washington, for the western section, and the Prairie Mountain 7.5 minute Quadrangle, Washington, for the eastern section.

The procedure followed was to choose easily recognizable points on the map, such as road intersections, and use these as base stations (Figures 9 and 10). Readings of the magnetic field at

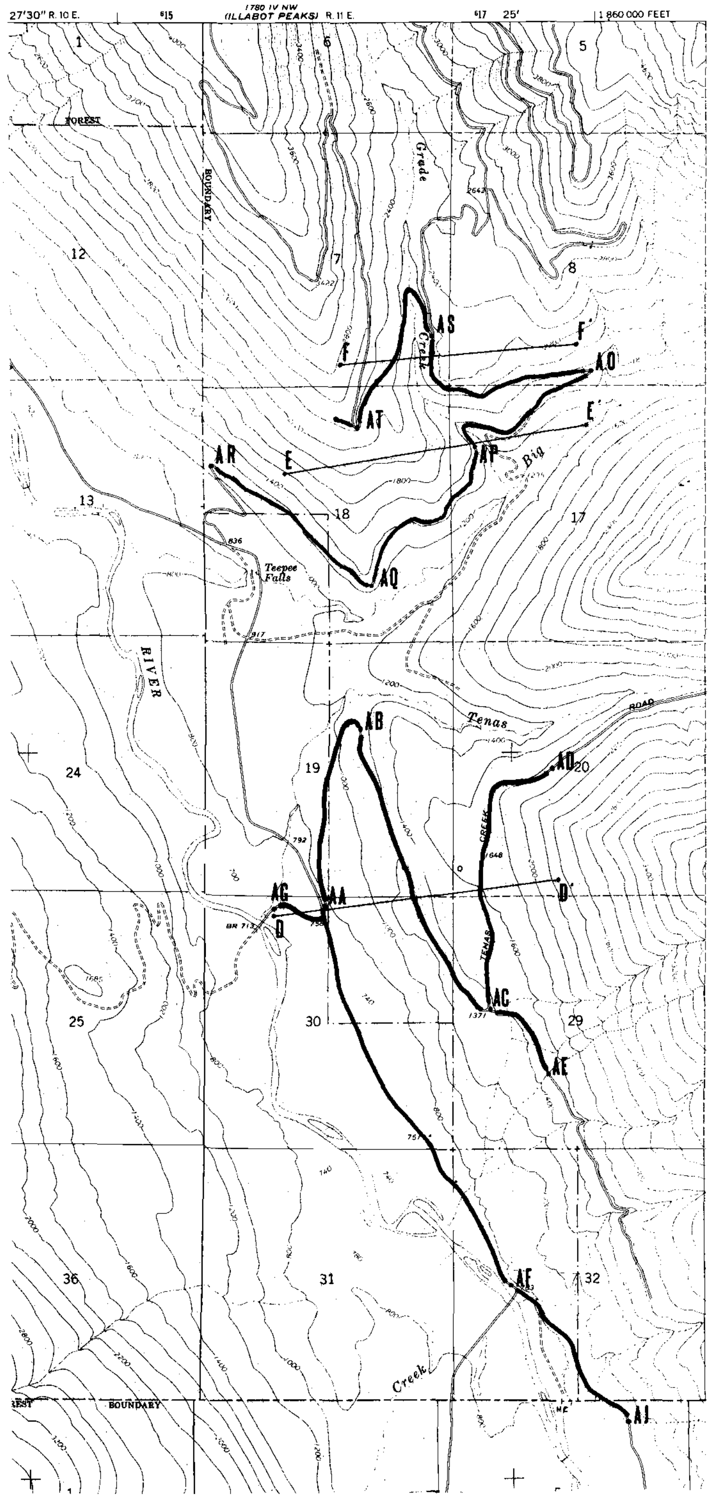

Figure 9. Eastern section, showing survey routes and base station locations.

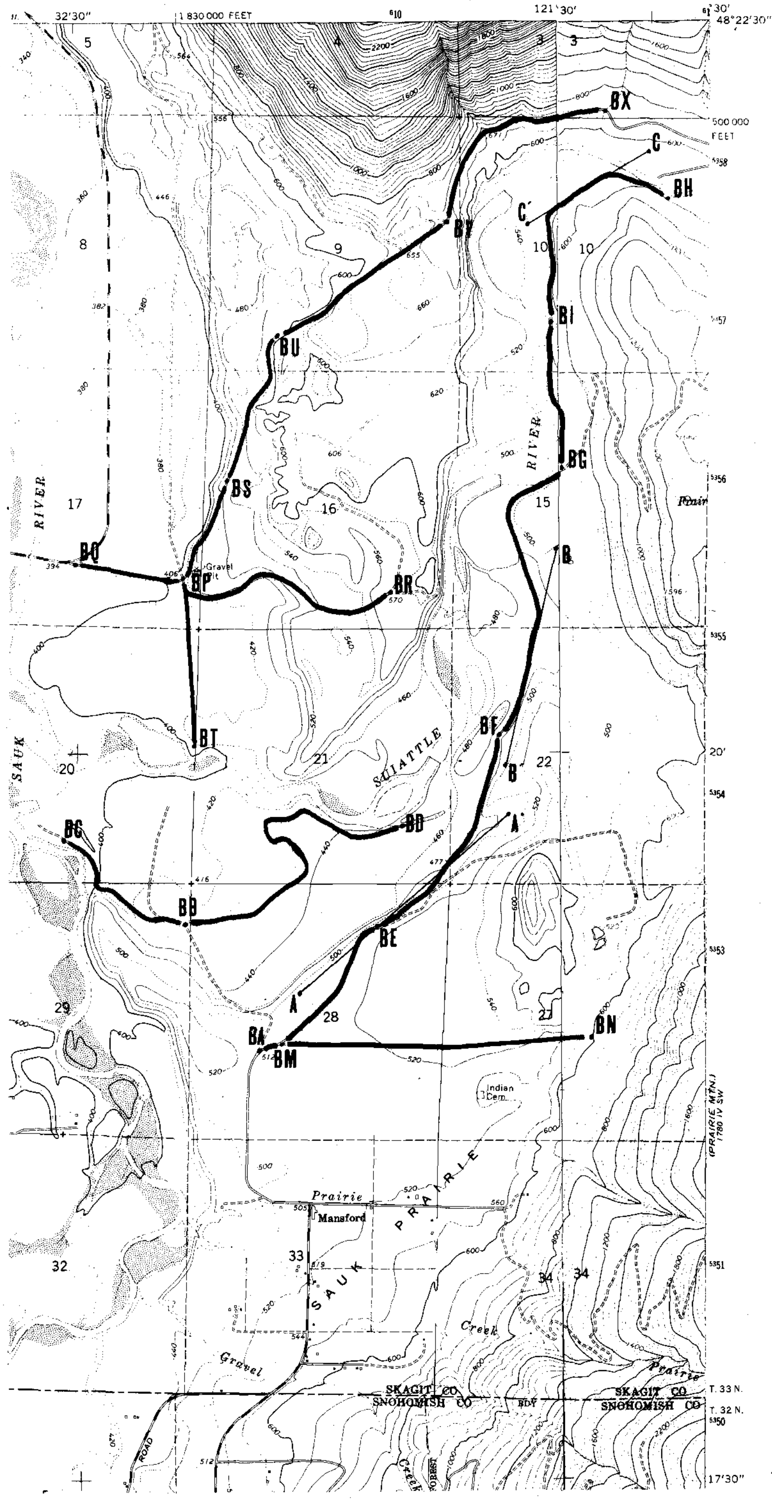

Figure 10. Western section, showing survey routes and base station locations.

one or more of these base stations were taken periodically throughout the day in order to be used for construction of graphs of the diurnal variation. Readings were taken every 100 paces along the road from one base station to the next base station. After returning to the first base station, another reading was taken. This method was followed throughout. Where possible, the first base station used on a given day was common to several survey lines run that day in order to better determine the diurnal variation. Furthermore, the investigator returned to certain base stations on other days of the survey, so that all readings, after correction for diurnal variation, were tied to the same base value.

Magnetic Data Reduction

Station Locations

Herein, each site at which a total field magnetic reading was taken is called a station, and each series of stations from one base station to the next base station is termed a section.

In the field, only the locations of the base stations and the routes surveyed were located on the base maps. Readings were taken every 100 paces along the survey route. The location of each station was obtained by using a map measure to measure the map distance along the survey route between consecutive base stations. This distance was then divided by the total number of paces between the base stations. Multiplying this distance by 100 yields the map distance between each station of the section. A programmable calculator was used to calculate the distance between each station of a given section and also the cumulative distance from the first base station to each successive station along the section.

These distances were then used to locate each station of the section on the base map.

Because several aspects of the data reduction and interpretation were accomplished using the CDC 3300 computer, the location of each station and base station had to be found to the nearest $1x10^{-4}$ degree latitude and longitude. This was accomplished by constructing latitude and longitude grid overlays at $50x10^{-4}$ and $3.3x10^{-4}$ degree intervals. Interpolation was used to obtain the nearest $10^{-4} \pm 5x10^{-5}$ degree latitude and longitude of the station.

Diurnal Variation Corrections

Corrections for diurnal variation were made in the field at the end of each day of surveying. A diurnal variation curve was constructed by plotting the readings at specific base stations verses time (Figures 11-13). Then a daily reference level was picked, usually the first reading at the main base station that day. In areas where the survey was continued for several days, the reference level was tied to one main base station. After the reference level was picked, each reading was adjusted to compensate for the diurnal variaion.

All of the daily variation curves as graphed were usable without further work, except the diurnal variation graph of 31 July 1976 (Figure 13a). On this date, no one base station was visited often enough during the day to give a good curve for the diurnal variation. A composite curve was therefore constructed (Figure 13b). This graph was constructed by plotting the average of each base station curve at 20 minute intervals. The first reading of the day at base station BA (Figure 10) was taken as the 0 gamma reference level. As each successive base station was first reached, the

(a)

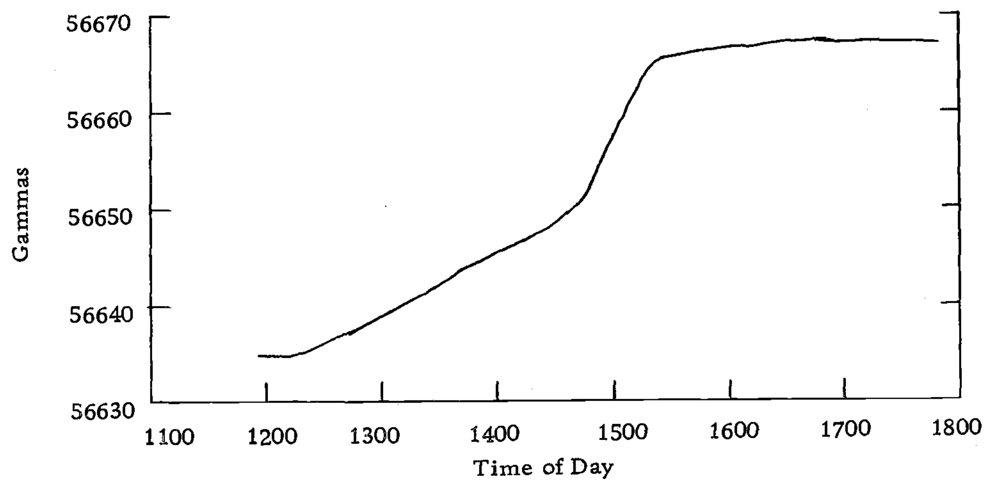

(b)

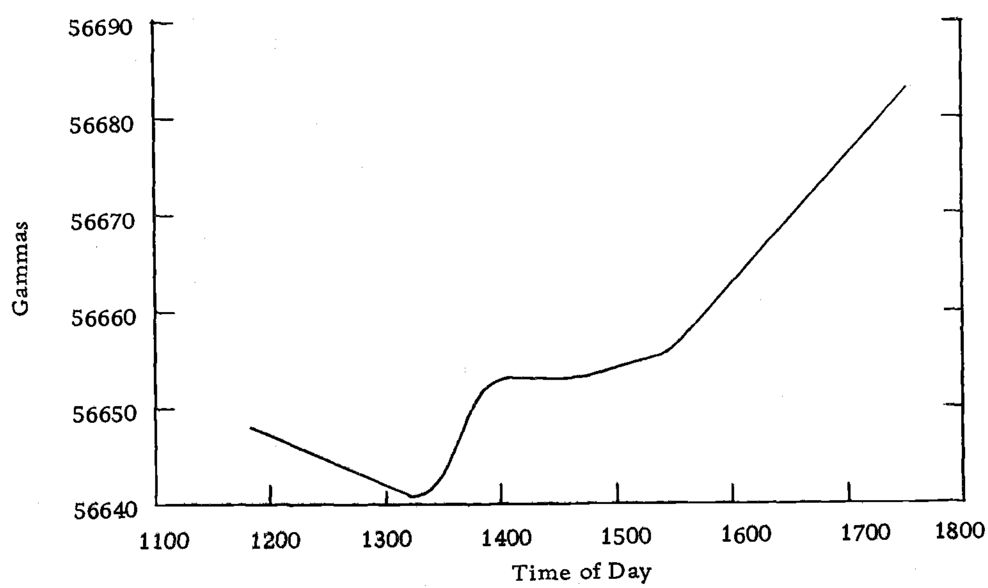

Figure 11. Diurnal variation curves. a. base station AA on 29 July 1976, b. base station AA on 30 July 1976.

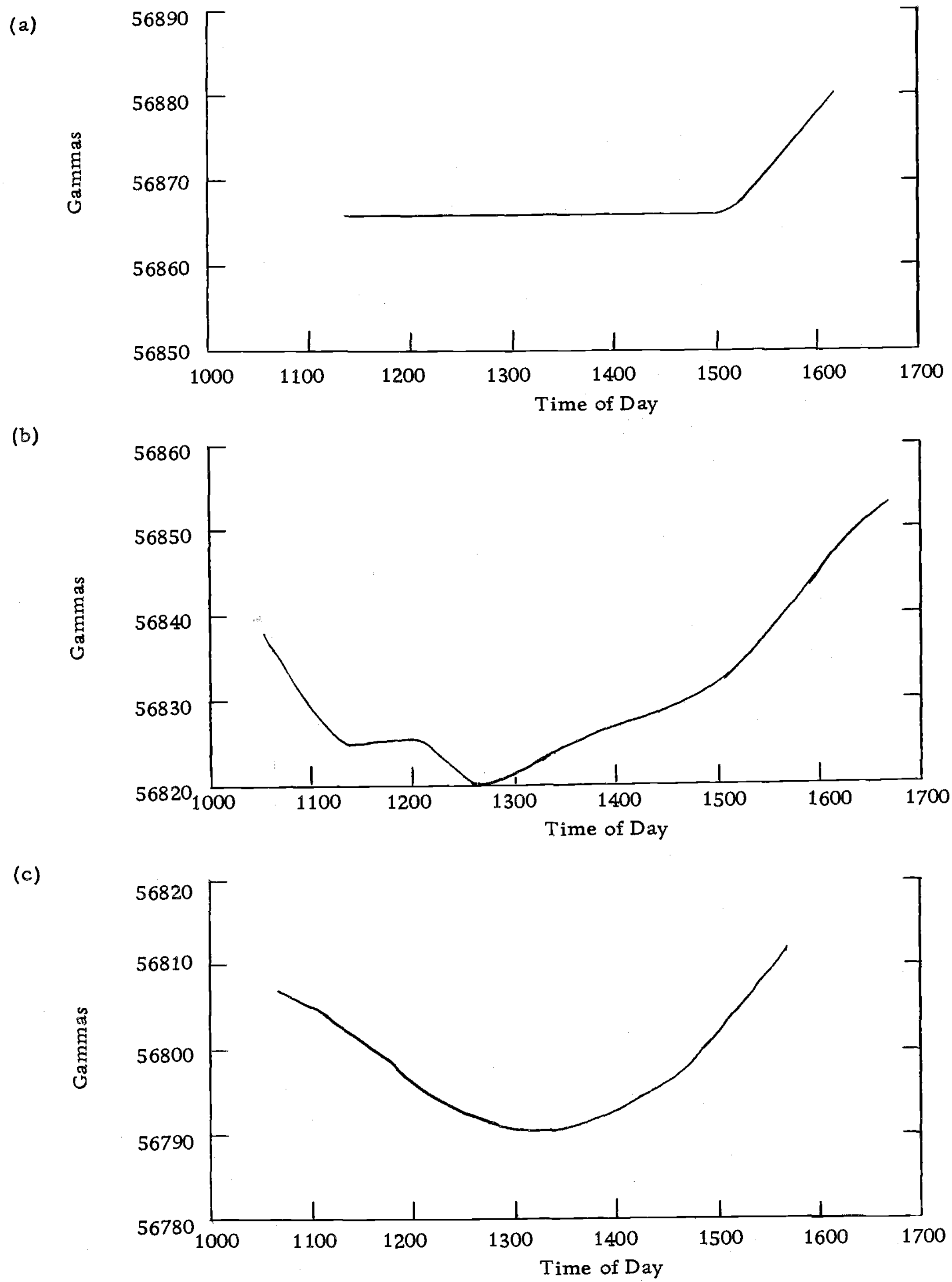

Figure 12. Diurnal variation curves. a. base station BA on 1 August 1976, b. base station BP on 2 August 1976, c. base station AO on 3 August 1976.

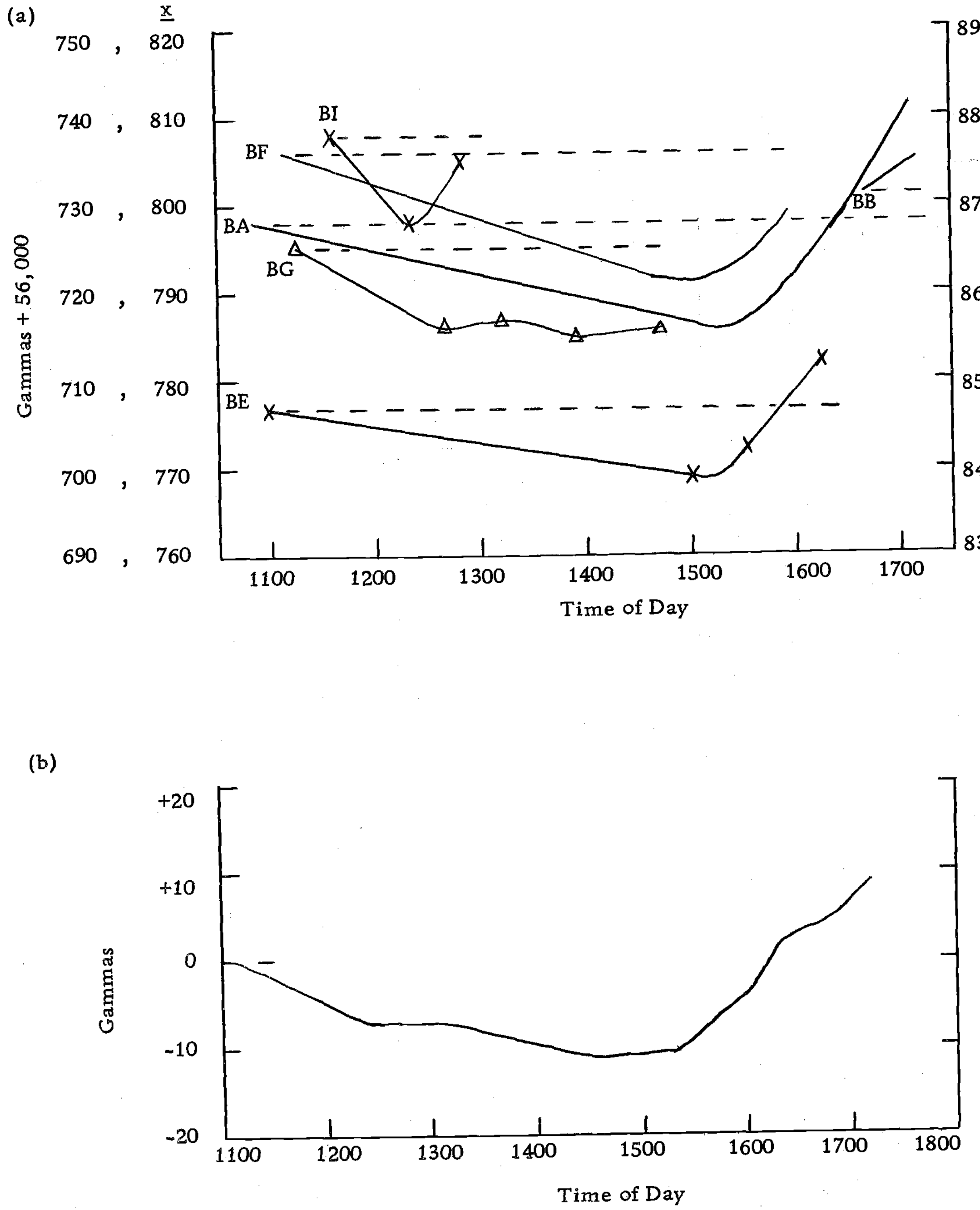

Figure 13. a. Diurnal variation curves at base stations BI, BF, BA, BG, BE, and BB on 31 July 1976. b. Composite diurnal variation curve for 31 July 1976.

initial reading was set equal to the composite curve constructed to that time. This first reading for each base station curve was set as the zero reference for that base station curve, for use in the determination of the amount of change at a specific time. These values were averaged to construct the composite diurnal variation curve.

Anomaly Computation

Anomalies are the variations between the magnetic field and the reference field given by equation 3-1.

$$\text{Anomaly} = \text{measured field} - \text{reference field} \qquad 3\text{-}1$$

The reference field used in this study is the International Geomagnetic Reference Field (IGRF), Epoch 1975. The IGRF for latitude 48°20'N and longitude 121°28'W was 56,751 gammas on July 30, 1976. The total field magnetic readings (corrected for diurnal variation), station designations, station locations, date of readings, and times of readings were entered into the CDC 3300. The anomaly was then computed and filed with the previous data.

Interpretive Methods and Interpretation: Western Section

Contour Map and Profiles

The CDC 3300 computer was used to plot the anomaly for each station on a mercator projection at a scale of 1 cm = 120 m. The plot of the western section was then hand contoured at ten gamma intervals by the investigator (Figure 14). The plot of data from the

Figure 14 Contour map of western section. Hand contoured at ten gamma intervals.

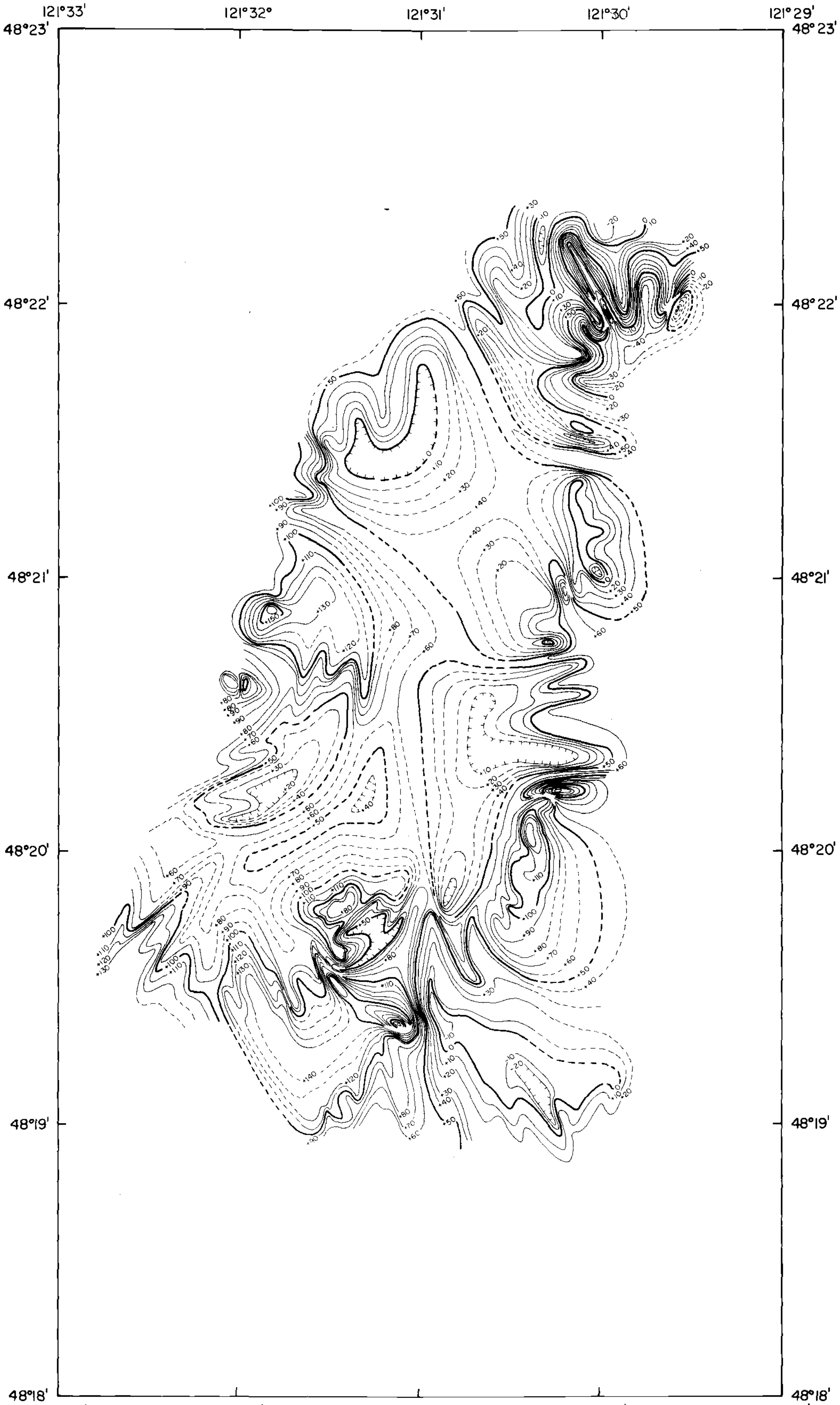
121°33'
121°32°
121°31'
121°30'
121°29'
48°23'
48°23'
48°22'
48°22'
48°21'
48°21'
48°20'
48°20'
48°19'
48°19'
48°18'
48°18'
121°33'
121°32'
121°31'
121°30'
121°29'

Figure 14

eastern section was not suitable for contouring because of insufficient data coverage.

Profile Construction

Three profiles were constructed from the contour map of the western section (Figure 10). These profiles were constructed where magnetic data density was greatest and showed marked anomalies (Figures 10 and 14).

Depth Determination

Depth to basement beneath the till was determined using the half-slope method of Peters (1947). This method involves the determination of the tangent of maximum slope to the anomaly. A line with one-half this maximum slope is tangent to the anomaly at two points. Both of these tangents were constructed, and the horizontal distance, h, between these two lines was measured. Then, the depth to basement s is given by formula 3-2

$$s = 1.6\,h \qquad (3\text{-}2)$$

This method is based on two assumptions: 1. that the anomalous mass is in the shape of an infinitely long slab of constant thickness with vertical sides and a horizontal top at depth h; and 2. this mass is uniformly magnetized in the vertical direction. This method was found generally to be accurate within $\pm$ 20% of the actual depth (Peters, 1947).

The depths determined for the major anomalies of profiles A-A', B-B', and C-C' are listed in Table 4. As shown in Table 4, the basement relief estimated from the major anomalies is

Table 4. Computed depth to bedrock.

Profile	Anomaly Position	Computed Depth	Model Depth	Model Depth Displaced 100 m East
A-A'	427m	112m	90m	105m
	610m	215m	150m	210m
	1310m	78m	120m	120m
B-B'	975m	170m	N/A	N/A
	1067m	61m		
	1280m	127m		
C-C'	152m	107m	N/A	N/A
	335m	156m		
	488m	132m		
	580m	93m		
	670m	115m		
	823m	141m		

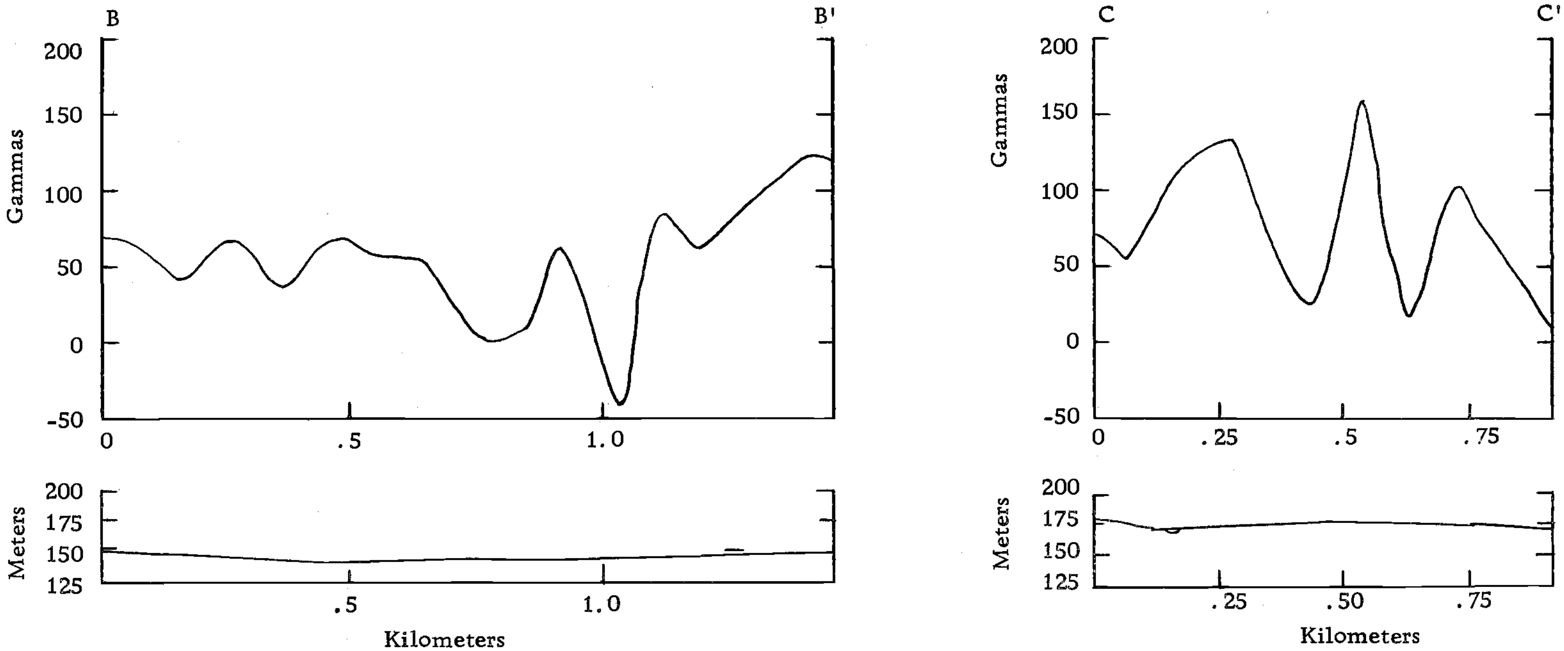

Figure 15. Magnetic and topographic profiles B-B' and C-C'.

approximately 140 m. The depths computed for profile C-C' might appear to be anomalously deep, because profile C-C' approaches within 180 m of bedrock exposure. But by continuing the slope of the hill to determine depth below C-C' at the closest approach to bedrock of profile C-C', a value of 170 m is obtained. This value is greater than any depth determined by Peters (1947) half-slope method for profile C-C'. The investigator also compared the computed depths for profile A-A' with model one, which is described later in this thesis (see Figure 16). This comparison is presented in Table 4. As Table 4 shows, the computed depth compares fairly well with the model depth. When the position of the anomaly center is offset 100 m to the east, the comparison between computed depth and model depth is much closer. Because magnetic anomalies are associated predominantly with edge effects, this offset is acceptable. It would appear that the depths are a reasonable approximation of basement depth, if the basement is composed of rocks with a uniform magnetic susceptability.

Magnetic Modeling

Profile A-A' was chosen for modeling, and two approaches to modeling were attempted. The first approach was to assume that the basement was of uniform magnetic susceptibility and that the observed anomalies were due to variations in basement relief. This approach was to determine the maximum basement relief. It was also to show if a fault was positively needed to produce the observed anomaly. The second approach was to assume that the basement was composed of blocks of differing magnetic susceptibilities, as might be found in a mélange, with a constant depth to basement. In actuality, the observed anomaly (A-A') is probably

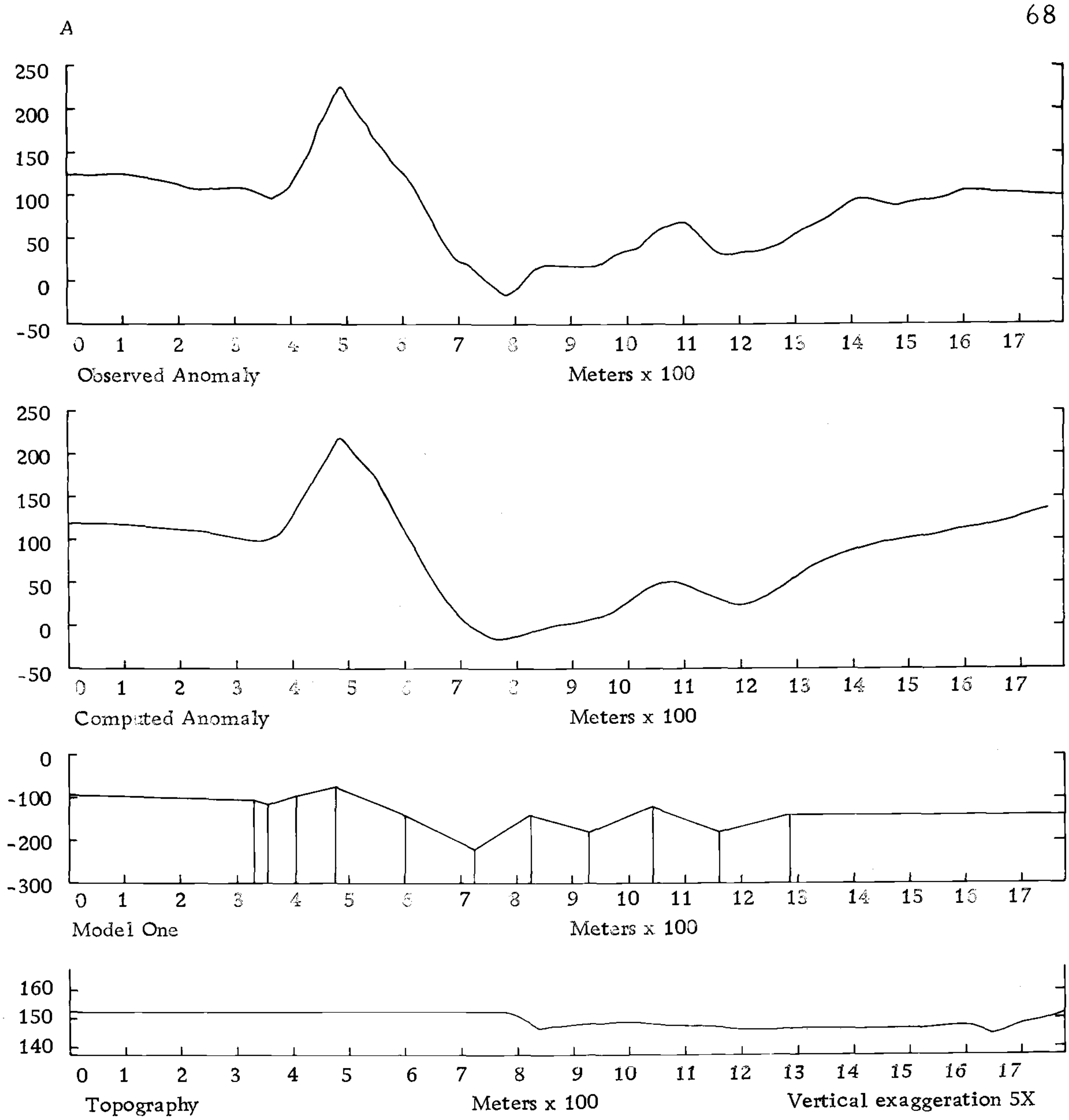

Figure 16. Model One: observed anomaly, computed anomaly, model one, and topographic profile, for profile A-A'.

the result of both a combination of basement relief and blocks of varying magnetic susceptibility.

Magnetic modeling was accomplished on the CDC 3300 computer using a program (*TWOMAG) developed by Richard J. Blakely (OSU). A listing of this program may be found in Appendix A. Program *TWOMAG calculated the total magnetic field anomaly over a series of two dimensional bodies. These bodies are assumed to have uniform magnetization and to be polygonal in cross section. The input data required to run *TWOMAG is listed in the program print-out in Appendix A. The procedure followed was to construct a profile model of consecutive polygons (Figure 16). This data was entered into the computer by punch cards and stored as a file. The file was listed and then run through *TWOMAG. The computer output from *TWOMAG was plotted on graph paper by the investigator and compared to the observed profile. Modifications were then made to the model to reduce the discrepancies between the observed profile and the computed profile. Usually, the file of the previous model could be changed in the edit mode of OS-3 to reflect the new model. When the discrepancies between the observed and computed profiles were too marked, a new model was entered on punch cards. This iterative method was followed until close agreement ($\pm$ 25 gammas) was obtained.

Model one (Figure 16) is based on the assumptions of approach one, i. e., the basement has a uniform magnetic susceptibility and the observed anomaly is the result of basement relief. Unfortunately, the data available in this area is restricted to the magnetic data the investigator obtained in the field, so a unique determination cannot be achieved. One point of reference used for the greatest depth of this model was the depth computed using Peters (1949) half-slope method. The magnetic susceptibility used originally was the computed magnetic susceptibility based on the volume percent of magnetite found in a thin section study of Chilliwack and meta-igneous samples. Formula 3-3 was used to compute the magnetic susceptibility, where

$$k = 2.89 \times 10^{-3} V^{1.01} \qquad 3\text{-}3$$

k is the computed magnetic susceptibility and V is the volume percent of magnetite (Dobrin, 1961). The volume percent of magnetite found in the Chilliwack and meta-igneous samples varied from zero to one percent, generally being less than one-half percent. For the first model attempted, a computed magnetic susceptibility of .00289 emu/cc was used based on one percent of magnetite. The anomaly computed was of the general form desired, but much too large. Because the volume percent of magnetite was quire variable and the magnetic susceptibility for one percent magnetite was too large, the depth estimate from the slope method was used. A magnetic susceptibility was found that resulted in a computed anomaly from the model of the correct amplitude. This magnetic susceptibility was .00145 emu/cc. This susceptibility is within the range of magnetic susceptibilities listed in Dobrin (1961) for sedimentary and metamorphic rocks. It is also compatible with the results of less than one percent magnetite obtained by the thin section study.

As can be seen in Figure 16, the anomaly computed from the model is very similar to the observed anomaly with a maximum difference of $\pm$ 25 gammas. In general, the difference is within $\pm$ 10 gammas of the maxima and minima of the observed anomaly. Furthermore, the computed anomaly and observed anomalies have similar slopes. Model one, which produced this computed anomaly, has a maximum depth of 220 m at 725 m from A. It has a minimum depth of 75 m at 475 m from A. Model one shows that the observed anomaly can be solely the result of basement relief for a basement of uniform magnetic susceptibility. The relief called for in the model is reasonable in this area and could represent pre-glacial stream channels and the topography between them. The model could also represent differential glacial erosion resulting from the movement of glaciers that deepened the Sauk Valley.

As stated previously, this is not a unique determination. The variables of the model used with limited constraints available are the depth to bedrock and the magnetic susceptibility. Also, the basic premise of uniform bedrock magnetic susceptibility is unlikely in the bedrock of the Sauk Prairie, as the rocks found directly to the east within 1.5 km of A' are of the mélange unit. For this reason, a second model was postulated.

This model assumes that the observed anomaly is caused by a basement of uniform depth composed of blocks of differing magnetic susceptibilities (see model two, Figure 17). This model is compatible with a mélange unit as bedrock and a glacially scoured up surface. Mélange has been defined as mappable bodies of deformed rocks characterized by the inclusion of native and exotic blocks, which may range up to several miles long, in a pervasively sheared, commonly pelitic matrix (Hsü, 1968). This describes the mélange unit of the Chilliwack and meta-igneous rocks of this area.

Model two is constructed of two rock types displaying different magnetic susceptibilities. Rock type one with a magnetic susceptibility of .00083 emu/cc represents the Chilliwack strata. Rock type two with a magnetic susceptibility of .00309 emu/cc represents the meta-igneous rocks. These values of magnetic susceptibility are averages obtained from Dobrin (1961). The type one susceptibility was obtained as an average for sedimentary rocks; the type two susceptibility was obtained as a combined average for

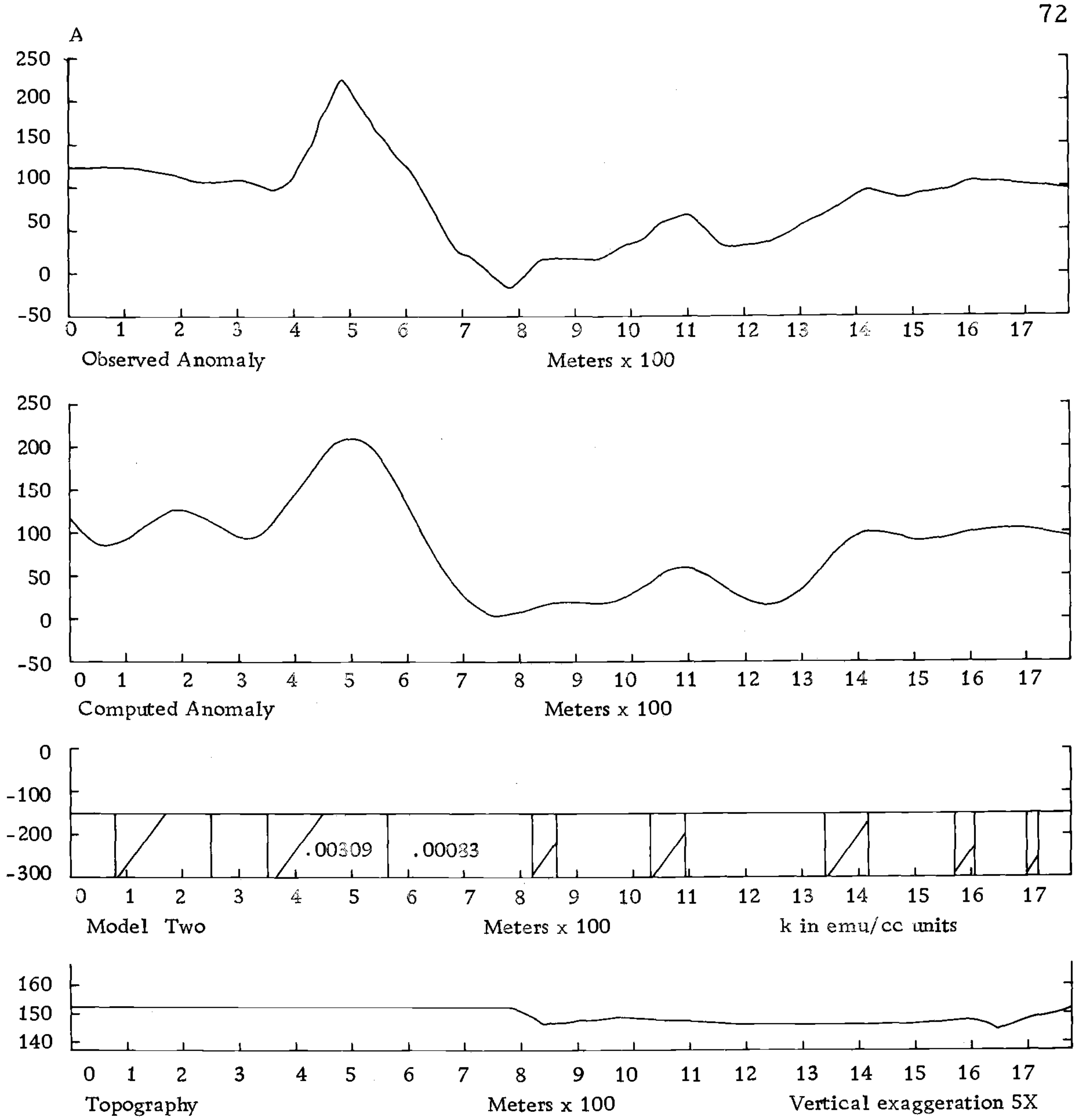

Figure 17. Model Two: observed anomaly, computed anomaly, model two, and topographic profile, for profile A-A'.

metamorphic and acid igneous rocks, since rock type two represents the meta-igneous rocks.

Model two produces a computed anomaly quite similar to the observed anomaly from 300 m to A' with a maximum variation of ± 20 gammas and an average variation of ± 10 gammas. The maxima and minima of the computed anomaly correspond to those of the observed anomaly. The slopes of the two anomalies also are very similar. From 300 m to A the computed anomaly has a greater variation. However, this discrepancy could have been reduced by assuming that this section of the model is a mixture of small Chilliwack and meta-igneous blocks. Model two includes a large meta-igneous block from 350 m to 565 m (215 m wide) and smaller blocks at 820 m to 865 m, 1,030 m to 1,095 m, 1,340 m to 1,415 m, 1,570 m to 1,605 m, and 1,700 to 1,720 m. Field work in the mélange unit of the thesis area suggests that this model is realistic. These size blocks have been observed and mapped in associations similar to those represented in model two.

Model two also is not a unique solution. The depth to basement was placed at 150 m, representing the average depth in model one. If the depth to basement were increased, the differences between magnetic susceptibilities necessary would have to be increased to produce the observed anomaly. Furthermore, much of the high frequency fluctuation would be lost. The magnetic susceptibilities represent averages for general rock types. While not inconsistent with the data from thin section studies, the magnetic susceptibilities could vary widely. Also, more susceptibilities are likely to be involved than those used in model two. Still an additional factor introducing uncertainty is that small blocks are involved. Each block has its own magnetic field, and the observed anomaly is the result of the superposition of the fields of the individual blocks.

Models one and two, although not unique, give an idea of what could cause the observed anomaly. The observed anomaly is most likely to be the result of blocks of both differing magnetic susceptibilities and basement relief. Model one sets a probable upper limit of 145 m on the amount of basement relief and an average depth to bedrock of 150 m $\pm$ 25 m. This model also shows where the maxima and minima of relief must occur to produce the observed anomaly. Model two sets the lower limit on basement relief at zero meters and shows that the observed anomaly can be the result solely of blocks of varying magnetic susceptibilities. The depth to bedrock used for this model was 150 m. This depth could not be much greater or the high frequency anomalies would be lost, at the same time the average depth could not be much less or the computed anomaly would be too large. This model shows where the blocks of higher magnetic susceptibility must be situated in relation to the blocks of lower magnetic susceptibility and the relative sizes of the blocks. Model one shows that a fault is not required to produce the observed anomaly. It does not, however, rule out the possibility that a fault caused the observed anomaly, because a fault is a probable locus of deep differential erosion.

Methods and Interpretation: Eastern Section

Profiles

Three composite profiles were constructed; D-D', E-E' and F-F' (Figures 18 and 19). All three profiles are perpendicular to the trend of the Straight Creek fault. The survey routes in this area followed the roads, which, of course, are not straight lines perpendicular to the Straight Creek fault, but are restricted to

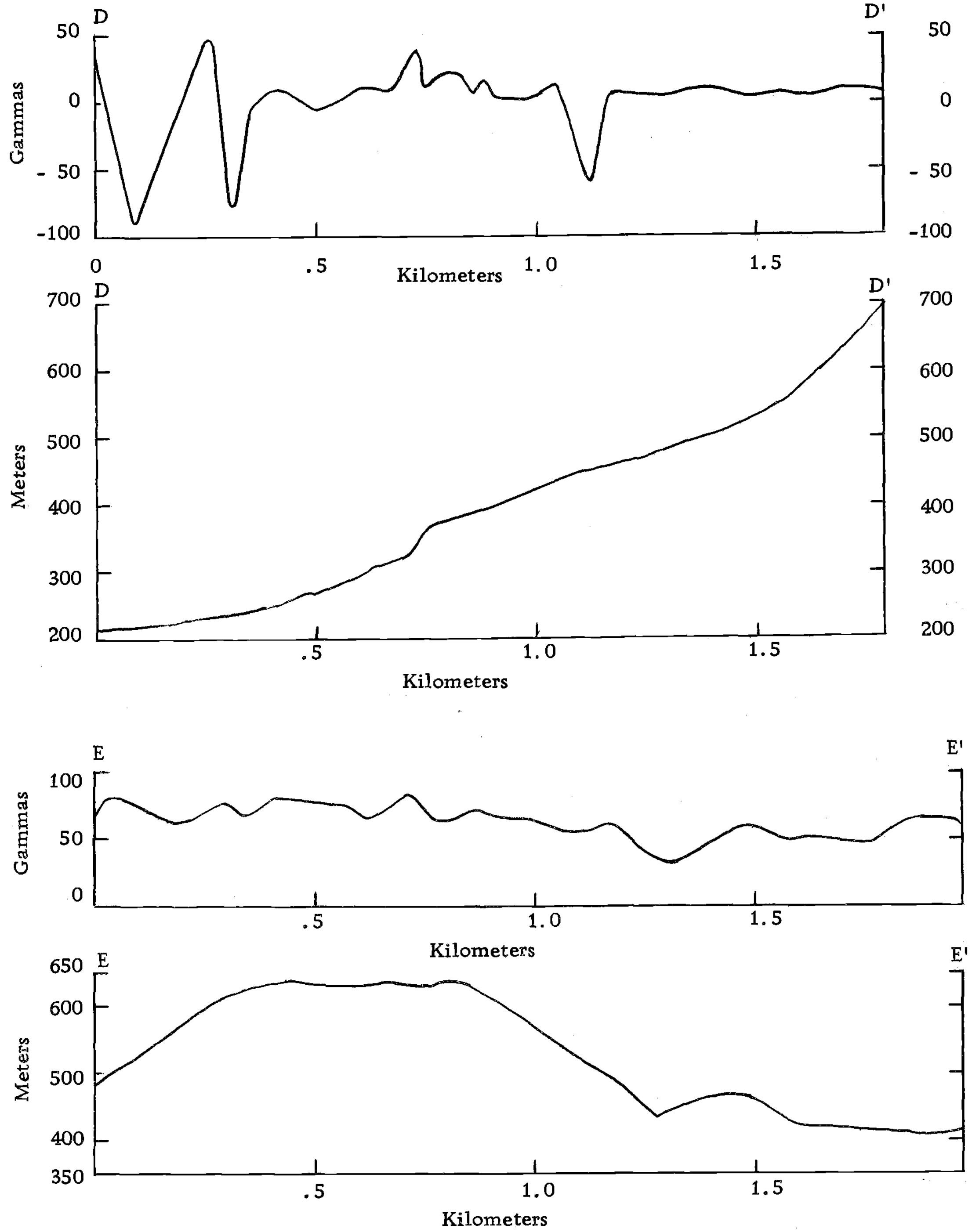

Figure 18. Profiles D-D' (top) and E-E' (bottom), with their topographic profiles below the anomaly profile.

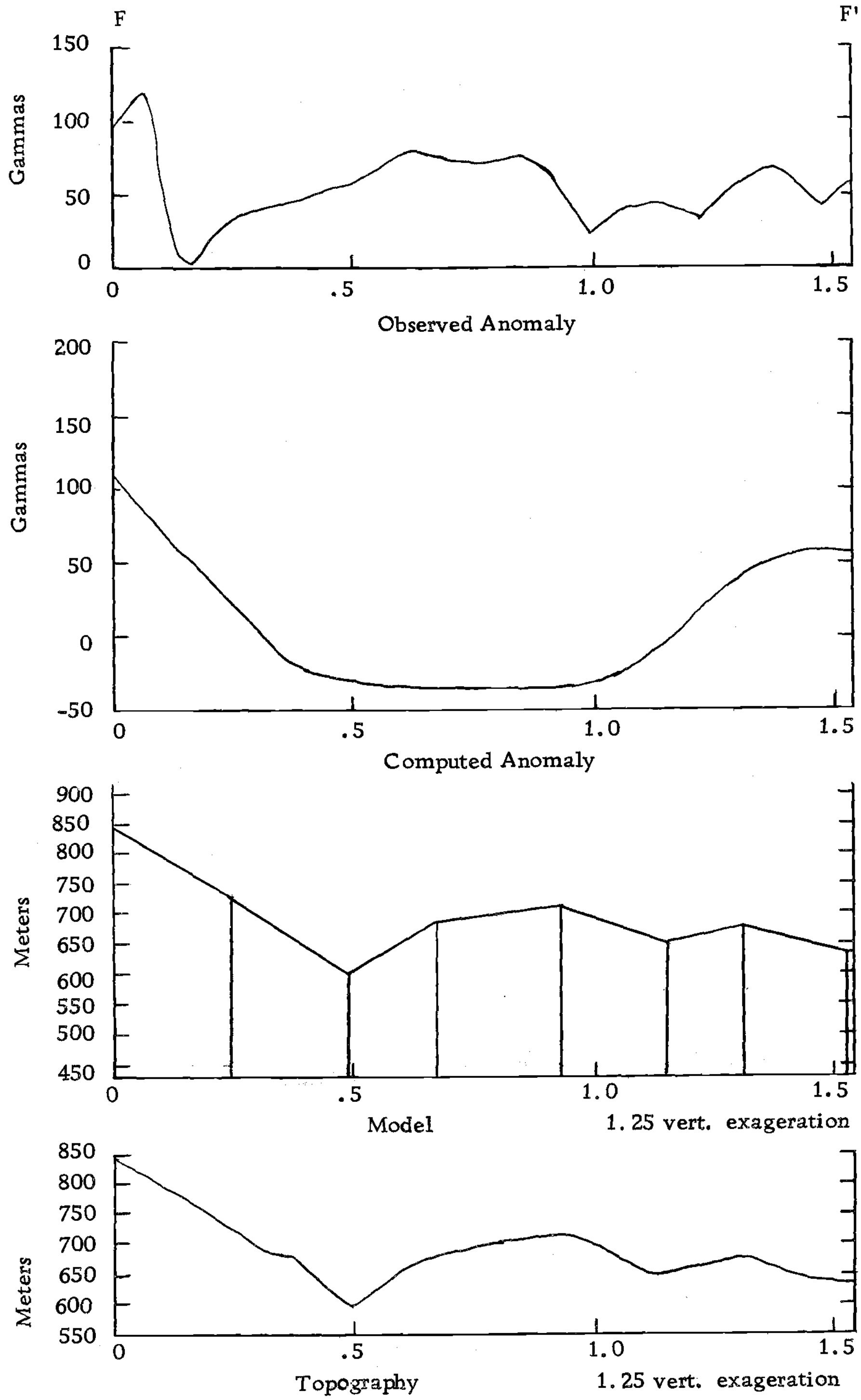

Figure 19. Model three: observed anomaly, computed anomaly model three, and topographic profile for profile F-F'.

acceptable grades (see Figure 9). In order to make straight profiles perpendicular to the trend of the Straight Creek fault, data was projected a short distance parallel to this trend. This method assumes that any major anomaly in this area is the result of juxtaposition of differing rock types across the fault. Also, that each rock unit is of a uniform magnetic susceptibility and is fairly continuous along the fault. Based on these assumptions, it follows that for any given distance from the fault, readings on a line parallel to the fault would have the same value. Following this reasoning, profiles were then constructed directly from these three lines using the migrated data.

When profiles D-D', E-E', and F-F' are compared (see Figures 18 and 19), they are obviously dissimilar. Profile D-D' has a large negative anomaly at 1,125 m east of D. This point is over the Straight Creek fault trace as determined from outcrops. During the field survey, the investigator noticed that the readings decreased rapidly (within a few feet) in all directions from this same point. Because of this, the anomaly is believed due to a buried pile of scrap metal. West of this position on the profile are high frequency variations with average amplitudes of 14 gammas. This is an area known to be of Shuksan Schist, while east of the Straight Creek fault at this position are the pre-Eocene intrusives. After the profile crosses the Straight Creek fault, very little variation occurs. This pattern is not repeated in profiles E-E' and F-F'. Profile F-F' crosses the Straight Creek fault where a tectonic sliver of Swauk strata separates the Shuksan Schist to the west and the Skagit Gneiss and the pre-Eocene intrusives to the east. Looking at this profile alone, the two large negative anomalies could represent the Straight Creek Fault. The negative anomaly at 150 m agrees well with the location of the western edge of the tectonic sliver of

Swauk strata determined from geological mapping. The eastern negative anomaly at 1, 000 m coincides with the eastern edge of the glacially covered bench. This appears to be a reasonable location for the eastern edge of the sliver of Swauk strata. A model (Figure 19) was made following this premise and using the land surface as the upperbound. The purpose of this model was to determine if the observed anomaly was the result of topography. Average magnetic susceptibilities for sedimentary rocks, metamorphic rocks, and igneous rocks were taken from Dobrin (1961). As can be seen in the computed anomaly for model three, the observed anomaly is not the result of relief alone. Another unit of higher magnetic susceptibility must be present under the glacial bench to account for the positive anomaly or the positive anomaly is caused by the glacial debris.

Based on the three profiles (D-D', E-E', and F-F') the investigator concludes that the Straight Creek fault in this area cannot be detected by a single magnetic signature. This was expected due to the juxtaposition of various rock types across the Straight Creek fault. A marked negative anomaly is the more likely signature to be found for the fault. It does appear possible to use the known magnetic signatures for the Straight Creek fault, in the thesis area, to determine rock types juxtaposed by the Straight Creek fault in covered areas.

CONCLUSIONS AND CONTRIBUTIONS

This thesis presents a geologic map of the area in greater detail than any previously presented. Results from this detailed mapping include a new location for the basal thrust of the Shuksan thrust system. The basal thrust is west of the Suiattle River, not under it in the thesis area as previously throught. A small block of Chilliwack strata, surrounded by greenschist is located in section 18, 3 km behind the basal Shuksan thrust. This gives strong support for a concave, upward, relatively shallow basal shuksan thrust, with mélange unit rocks present at approximately 200 m $\pm$ 150 m below sea level at this location.

Petrographic study showed that the "All Creek Volcanics" is a block of the meta-igneous rocks (Paleozoic age) that is predominantly composed of volcanics and is not a separate unit of Tertiary age. Also, grains of the meta-igneous rocks found in the Chilliwack strata indicate that the meta-igneous rocks were a partial source for the Chilliwack strata. Furthermore, the conglomerate at the top of the "All Creek Volcanics" meta-igneous block is in depositional contact, not tectonic contact, with the meta-igneous rocks below it and probably represents the basal Chilliwack conglomerate. In addition, a limestone pod found in section 14 contains probable fossils of foraminiferas.

The magnetic study gives an idea of the subsurface geology of the Sauk Prairie and a more precise location for the trace of the Straight Creek fault.

The sedimentary study of the Chilliwack strata show that the sandstones are lithic wackes and suggest a deepsea fan as the likely depositional environment, while the study of the meta-igneous rocks indicates that they are fragments of oceanic crust from an intra-arc basin. The comparative study of the Chilliwack, Swauk, and Nooksack sandstones suggests an island arc depositional site for the Chilliwack and Nooksack sandstone and a continental depositional site for the Swauk sandstones. It is probable that the Chilliwack strata, in the thesis area, was deposited as a deepsea fan building eastward off of an island arc into an intra-arc basin.

BIBLIOGRAPHY

Breiner, S., 1973, Applications manual for portable magnetometers: GeoMetrics, Palo Alto, Cal., 58 p.

Bostwick, 1977, Personal communication.

Brown, E. H., 1974, Comparison of the mineralogy and phase relations of blueschist from the North Cascades, Washington, and greenschists from Otago, New Zealand: G. S. A. Bull., v. 85, p. 333-344.

Bryant, B. H., 1955, Petrology and reconnaissance geology of the Snowking area, Northern Cascades, Washington: unpublished Ph. D. thesis, University of Washington, 352 p.

Crowder, D. F., Tabor, R. W., and Ford, A. B., 1969, Geologic map of the Glacier Peak quadrangle, Snohomish and Chelan counties, Washington: U. S. Geol. Survey Geol. Quad. Map CQ-473.

Daly, R. A., 1912, Geology of the North American Cordillera at the 49th parallel: Geol. Survey of Canada Memoir 38, pt. 1, p. 508-516.

Danner, W. R., 1966, Limestone resources of western Washington: Washi ngton Div. Mines and Geology Bull. 52.

Dickinson, W. R., 1970, Interpreting detrital modes of graywacke and arkose: Jour. Sed. Pet., v. 40, no. 2, p. 695-707.

________________. 1972, Evidence for plate-tectonic regimes in the rock record: American Jour. of Science, v. 272, p. 551-576.

________________, 1976, Paleocurrent trends and petrologic variations in Mesozoic strata near South Fork of John Day River, Central Oregon: G. S. A. Abs. with Prog., v. 8, no. 3, p. 368-369.

Dobrin, M. B., 1960, Introduction to geophysical prospecting: McGraw-Hill, New York, 446 p.

Ernst, W. G., 1972, Occurrance and mineralogic evolution of blue-schist belts with time: American Jour. of Science, v. 272, p. 657-668.

Folk, R. L., 1962, Spectral subdivision of limestone types: Amer. Assn. Pet. Geol. Mem. no. 1, p. 62-84.

Foster, Robert, 1960, Tertiary geology of a portion of the central Cascades mountains, Washington: G. S. A. Bull., v. 71, p. 99-126.

Franklin, W. E., 1974, Structural significance of meta-igneous fragments in the Prairie Mountain area, North Cascade range, Snohomish county, Washington: Unpublished M. S. thesis, Oregon State University, 109 p.

Geotimes, 1973, Plutonic rocks, classification and nomenclature recommended by the IUGS subcommission on the systematics of igneous rocks: v. 13, no. 10, p. 26-30.

Grant, A. R., 1969, Chemical and physical controls for base metal deposition in the Cascade Range of Washington: Washington Div. Mines and Geology Bull. 58.

Higgins, M. W., 1971, Cataclastic rocks: USGS Professional paper 683.

Hsü, K. J., 1968, Principles of mélanges and their bearing on the Franciscan-Knoxville paradox: G. S. A. Bull., v. 79, p. 1063-1074.

__________, 1971, Franciscan melanges as a model for eugeo-synclinal sedimentarion and underthrusting tectonics: Jour. Geophys. Research, no. 5, p. 1162-1170.

Huntting, M. T., Bennett, W. A. G., Livingston, V. E., and Moen, W. S., Compiled 1961, Geologic Map of Washington: Wash. Div. Mines and Geology.

Jenne, David A., OSU, Thesis in progress.

Johnson, S. H., and Couch, R. W., 1970, Crustal structure in the North Cascade Mountains of Washington and British Columbia from seismic refraction measurements: Seismol. Soc. Amer. Bull., v. 60, p. 1259-1269.

Karig, D. E., 1971, Origin and development of marginal basins in the western basins of the Western Pacific: J. G. R., v. 76, no. 11, p. 2542-2560.

______________, 1972, Remnant arcs: G. S. A. Bull., v. 83, p. 1057-1068.

Lawrence, R. D., 1972, Plate tectonic interpretation of major structures, Northern Cascade Range, Washington: unpublished manuscript.

______________, 1977, Personal communication.

Mackin, J. H., and Cary, A. S., 1965, Origin of Cascade landscapes: Wash. Div. Mines and Geology, Information Circular no. 41, 35 p.

Mattinson, J. M., 1970, Uranium-led geochronology of the northern Cascade Mountains; Washington (abstr.): Geol. Soc. America Abstr., v. 2, p. 116.

______________, 1972, Ages of zircons from the Northern Cascade Mountains, Washington: Geol. Soc. America Bull., v. 83, p. 3769-3784.

McTaggart, K. C., 1970, Tectonic history of the Northern Cascades Mountains, in J. O. Wheeler (ed.), Structure of the Southern Canadian Cordillera: Geol. Assoc. Canada Sp. Paper 6, p. 137-148.

Milnes, P. T., 1977, Structural geology and metamorphic petrology of the Illabot Peaks area, Skagit county, Washington: unpublished M. S. thesis, Oregon State University, 118 p.

Misch, Peter, 1966, Tectonic evolution of the Northern Cascades of Washington state; H. C. Gunning, and W. H. White (eds.), Tectonic history and mineral deposits of the western Cordillera: Canadian Inst. Mining and Metallurgy Spec. v. 8, p. 101-148.

______________, 1977, Dextral displacements at some major strike faults in the North Cascades: Geological and Mineralogical Assoc. of Canada Abs. with Prog., v. 2, p. 37.

Miyashiro, Akiho, 1972, Metamorphism and related magmatism in plate tectonics: American Jour. Science, v. 272, p. 629-657.

Nelson, C. H., Kulm, L. D., 1973, Submarine fans and deep-sea channels, in Turbidites and deep water sedimentation, SEPM Pacific Section Short Course, Los Angeles, p. 39-78.

Normark, W. R., 1973, Submarine canyons and fan valleys: factors affecting growth processes of deep-sea fans: In Dott, R. H., ed., Modern and ancient geosynclinal sedimentation: Soc. Econ. Paleo, and Min., Spec. Pub., p. 56-68.

Oxburgh, E. R., and Turcotte, D. L., 1971, Origin of paired metamorphic belts and crustal dilation in island arc regions: J.G.R., v. 76, no. 5, p. 1315-1327.

Peters, L. J., 1949, The direct approach to magnetic interpretation and its practical applications: Geophysics, v. 14, p. 290-320.

Pettijohn, F. J., Potter, P. E., and Siever, Raymond, 1972, Sand and Sandstone: Springer-Verlag, New York, 618 p.

Spry, Alan, 1969, Metamorphic textures: Pergamon Press Inc., New York, 350 p.

Tabor, R. W., 1961, The crystalline geology of the area south of Cascade Pass, northern Cascade Mountains, Washington: unpublished Ph.D. thesis, University of Washington, 259 p.

_______________, and Crowder, D. F., 1969, On batholiths and volcanoes-intrusion and eruption of Late Cenozoic magmas in the Glacier Peak area, North Cascades, Washington: U.S. Geol. Survey Prof. Paper 604, 63 p.

Vance, J., 1957, The geology of the Sauk River area in the Northern Cascades of Washington: unpublished Ph.D. thesis, University of Washington, 312 p.

_______________, 1974, Mid-Palezoic stratigraphy and metamorphism in NW Washington: G.S.A. Abs. with Prog., v. 6, no. 3, p. 269.

Wager, L. R., Brown, G. M., 1967, Layered igneous rocks: W. H. Freeman, San Francisco, 630 p.

Williams, H., Turner, F. J., and Gilbert, C. M., 1954, Petrography: An introduction to the study of rocks: W. H. Freeman, San Francisco, 406 p.

Yeats, R. S., Crystalline klippen in the Index District, Cascade Range, Washington: G.S.A. Bull., v. 75, p. 549-562.

APPENDICES

APPENDIX A

Appendix A

```
      PROGRAM TWOMAG
C
      DIMENSION HX(2000),HZ(2000),HT(2000),X(2000)
      REAL MI,MD,M,JX,JZ,JXP,JZP
C
C*************************************************************************
C
C        PROGRAM TWOMAG COMPUTES THE HORIZONTAL, VERTICAL, AND TOTAL FIELD
C     ANOMALY PROFILES PRODUCED BY ONE OR MORE TWO-DIMENSIONAL MAGNETIC
C     BODIES WITH ARBITRARY CROSS-SECTIONAL SHAPE.  ASSUMPTIONS
C     ARE (1) THE BODY IS INFINITELY EXTENDED IN THE PLUS AND
C     MINUS Y DIRECTIONS, (2) EACH BODY IS UNIFORMLY MAGNETIZED,
C     AND (3) EACH BODY CAN BE APPROXIMATED BY A POLYGON.
C        PROGRAM WRITTEN BY RICHARD J. BLAKELY, SCHOOL OF OCEAN-
C     OGRAPHY, OREGON STATE UNIVERSITY, CORVALLIS, OREGON 97331.
C     LAST UPDATE WAS MADE ON SEPTEMBER L16, 1975.
C
C
C   INPUTS -
C
C       EACH RUN REQUIRES THE FOLLOWING DATA ON ONE CARD (FMT 2I5,7F10.1)...
C        NX -      THE NUMBER OF DATA POINTS REQUIRED.
C        IPUNCH - IF IPUNCH = 1, THE TOTAL FIELD ANOMALY WILL BE PUNCHED
C                 ON CARDS.  IF IPUNCH = 0, NO ACTION.
C        XSTART - THE STARTING X-COORDINATE (KM).
C        XDELT -  THE SPATIAL SAMPLE INTERVAL (KM).
C        MI -     THE INCLINATION OF THE MAGNETIZATION OF THE SOURCE
C                 (DEGREES).
C        MD -     THE DECLINATION OF THE MAGNETIZATION.
C        FI -     THE INCLINATION OF THE REGIONAL FIELD.
C        FD -     THE DECLINATION OF THE REGIONAL FIELD.
C        TREND -  THE TREND OF THE TWO-DIMENSIONAL SOURCE.
C
C       EACH BODY REQUIRES THE FOLLOWING DATA ON ONE CARD (FMT I5,F10.1)...
C
C        NSIDES - THE NUMBER OF SIDES TO THE PRISM.
C        M -      THE MAGNITUDE OF THE MAGNETIZATION (EMU/CC).
C
C       EACH CORNER OF THE BODY REQUIRES THE FOLLOWING DATA
C       ON ONE CARD (FMT(2F10.1)...
C
C        X2 -     THE X COORDINATE (KM).
C        Z2 -     THE Y COORDINATE.
C
C
C     NOTE 1 - THE COORDINATES OF THE CORNERS SHOULD BE TAKEN CLOCKWISE.
C              FOR EXAMPLE, THE DATA REQUIRED (NSIDES,M,X1,Z1) FOR A
C              UNIT-SQUARE BODY AT 1 KM DEPTH ARE AS FOLLOWS...
C
C      4       .005
C         -.5        .5
C           .5       .5
C           .5      1.5
C         -.5       1.5
C               (BLANK)
C
C     NOTE 2 - ONE BLANK CARD TERMINATES THE PROFILE AND A NEW PROFILE
C              IS INITIATED; TWO BLANK CARDS TERMINATE THE PROGRAM.
C
C     NOTE 3 - THE PARAMETER [TREND[ DETERMINES THE DIRECTION OF THE
C              PROFILE TRACK AS FOLLOWS.  [TREND[ DETERMINES THE POSITIVE
```

```
C            Y DIRECTION, Z IS POSITIVE DOWNWARD, AND THE X-AXIS IS IN
C            THE SENSE OF A RIGHT HANDED SYSTEM.  THE PROFILE IS TAKEN
C            IN THE POSITIVE X-DIRECTION.
C   NOTE 4 - LOGICAL UNITS ARE... 5 = CARD INPUT
C                                 6 = LINE PRINTER OUTPUT
C                                 7 = CARD PUNCH.
C   NOTE 5 - IN SUBROUTINE RIBBON, A FUNCTION CALLED ARCTAN IS
C            USED WHICH IS DIFFERENT THAN THE STANDARD
C            FUNCTION ATAN2.  ARCTAN(X,Y) IS DEFINED AS
C            ARCTAN(Y/X) AND IS EQUIVALENT TO ATAN2(Y,X).
C
C***********************************************************************
C
      WRITE(6,108)
  108 FORMAT(1H1)
 1002 READ(5,100)NX,IPUNCH,XSTART,XDELT,MI,MD,FI,FD,TREND
  100 FORMAT(2I5,7F10.1)
      IF(NX.EQ.0)GO TO 1003
      KLAB=0
      WRITE(6,102)NX,IPUNCH,XSTART,XDELT,MI,MD,FI,FD,TREND
  102 FORMAT(///,' INPUT TO TWOMAG...',//,10X,'NX = ',I5,/,10X,'IPUNCH =
     1 ',I5,/,10X,'XSTART = ',F10.1,/,10X,'XDELT = ',F10.1,/,10X,'MI = '
     2,F10.1,/,10X,'MD = ',F10.1,/,10X,'FI = ',F10.1,/,10X,'FD = ',F10.1
     3,/,10X,'TREND = ',F10.1////)
      CONV=3.14159/180.
      MI=MI*CONV
      MD=MD*CONV
      FI=FI*CONV
      FD=FD*CONV
      TREND=TREND*CONV
      JXP=-COS(MI)*SIN(MD-TREND)
      JZP=SIN(MI)
      A=-COS(FI)*SIN(FD-TREND)
      B=SIN(FI)
      DO 1 I=1,NX
      HX(I)=HZ(I)=HT(I)=0.
    1 X(I)=XSTART+XDELT*FLOAT(I-1)
 1000 READ(5,106)NSIDES,M
  106 FORMAT(I5,F10.1)
      IF(NSIDES.EQ.0)GO TO 1001
      KLAB=KLAB+1
      WRITE(6,107)KLAB,M
  107 FORMAT('   BLOCK NUMBER ',I5,'     M = ',E10.3,//,8X,'X1',8X,'Z1',
     1//)
      JX=JXP*M
      JZ=JZP*M
      NT=NSIDES+1
      DO 2 J=1,NT
      IF(J.NE.1)GO TO 6
      READ(5,101)X2,Z2
      WRITE(6,101)X2,Z2
  101 FORMAT(2F10.1)
      XT=X2
      ZT=Z2
      GO TO 2
    6 CONTINUE
      IF(J.NE.NT)GO TO 7
      X1=X2
      Z1=Z2
      X2=XT
      Z2=ZT
```

```
      GO TO 8
    7 CONTINUE
      X1=X2
      Z1=Z2
      READ(5,101)X2,Z2
      WRITE(6,101)X2,Z2
    8 CONTINUE
      DO 3 I=1,NX
      CALL RIBBON(X(I),0.,X1,Z1,X2,Z2,JX,JZ,FX,FZ)
      FT=A*FX+B*FZ
      HX(I)=HX(I)+FX
      HZ(I)=HZ(I)+FZ
    3 HT(I)=HT(I)+FT
    2 CONTINUE
      GO TO 1000
 1001 WRITE(6,103)
  103 FORMAT(//,'  RESULTS OF TWOMAG',//,3X,'STATION',2X,'LOCATION',9X,
     1'X',9X,'Z',5X,'TOTAL'/)
      DO 5 I=1,NX
    5 HT(I)=HT(I)*10.**5
      WRITE(6,104)(I,X(I),HX(I),HZ(I),HT(I),I=1,NX)
  104 FORMAT(I10,4E10.3)
      IF(IPUNCH.NE.1)GO TO 4
      WRITE(7,105)(HT(I),I=1,NX)
  105 FORMAT(8F8.0)
    4 CONTINUE
      GO TO 1002
 1003 STOP
      END
      SUBROUTINE RIBBON(X0,Z0,X1,Z1,X2,Z2,JX,JZ,FX,FZ)
      REAL JX,JZ
C
C      SUBROUTINE RIBBON COMPUTES THE X AND Z COMPONENTS (FX,FZ) AT SOME
C    POINT (X0,Z0) DUE TO A RIBBON INFINITE IN THE Y-DIRECTION AND
C    BOUNDED IN THE X-Z PLANE BY (X1,Z1) AND (X2,Z2).  THE MOMENT OF THE
C    RIBBON IS DETERMINED BY THE MAGNETIZATION VECTOR (JX,JZ) , THE MAG-
C    NETIC MEDIA BEING CLOCKWISE TO THE VECTOR FROM (X1,Z1) TO (X2,Z2).
C
      SX=X2-X1
      SZ=Z2-Z1
      S=SQRT(SX**2+SZ**2)
      SX=SX/S
      SZ=SZ/S
C
      QS=JX*SZ-JZ*SX
C
      R1X=X1-X0
      R1Z=Z1-Z0
      R2X=X2-X0
      R2Z=Z2-Z0
      R1=SQRT(R1X**2+R1Z**2)
      R2=SQRT(R2X**2+R2Z**2)
C
      T1=ARCTAN(R1X,R1Z)
      T2=ARCTAN(R2X,R2Z)
C
      FS=2.*QS*ALOG(R1/R2)
      FN=2.*QS*(T1-T2)
C
      FX=FN*SZ+FS*SX
      FZ=-FN*SX+FS*SZ
      RETURN
      END
```

APPENDIX B

Appendix B. Table 1. Magnetic survey routes, section identifications and number of stations in each section excluding base stations.

Survey Routes Base Stations From	To	Section Identification	Number of Stations in Section Excluding Base Stations
BE	BA	BE	12
BE	BF	BF	18
BG	BF	BG	21
BM	BN	BM	22
BP	BT	BP	11
BP	BR	BR	16
BB	BD	BB	38
BB	BC	BC	11
BP	BQ	BQ	7
BP	BS	BS	7
BU	BS	BU	12
BU	BV	BV	14
BI	BS	BI	10
BI	BH	BH	15
BX	BV	BX	13
AA	AG	AG	3
AA	AF	AA	30
AA	AB	AB	15
AC	AD	AD	20
AC	AB	AC	23
AC	AE	AE	6
AP	AQ	AP	14
AS	AO	AS	16
AS	AT	AT	16
AQ	AR	AR	14
AP	AO	AO	12
AF	AJ	AF	14

Appendix A

BE00	07,31,76	1500	48.3238N	-121.5168W	56780	29
BE01	07,31,76	1502	48.3234N	-121.5182W	56906	155
BE02	07,31,76	1504	48.3227N	-121.5187W	56973	122
BE03	07,31,76	1501	48.3220N	-121.5193W	56835	84
BE04	07,31,76	1506	48.3213N	-121.5195W	56839	88
BE05	07,31,76	1507	48.3206N	-121.5200W	56845	94
BE06	07,31,76	1508	48.3199N	-121.5206W	56829	78
BE07	07,31,76	1509	48.3194N	-121.5215W	56846	95
BE08	07,31,76	1511	48.3184N	-121.5224W	56862	111
BE09	07,31,76	1512	48.3182N	-121.5232W	56833	82
BE10	07,31,76	1513	48.3178N	-121.5242W	56848	97
BE11	07,31,76	1514	48.3173N	-121.5248W	56856	105
BE12	07,31,76	1516	48.3169N	-121.5259W	56869	118
BA00	07,31,76	1517	48.3166N	-121.5270W	56869	118
BF01	07,31,76	1534	48.3243N	-121.5158W	56739	-12
BF02	07,31,76	1535	48.3247N	-121.5150W	56770	19
BF03	07,31,76	1536	48.3252N	-121.5142W	56768	17
BF04	07,31,76	1537	48.3256N	-121.5134W	56783	32
BF05	07,31,76	1538	48.3260N	-121.5124W	56810	59
BF06	07,31,76	1540	48.3266N	-121.5117W	56788	37
BF07	07,31,76	1514	48.3274N	-121.5111W	56791	40
BF08	07,31,76	1542	48.3279N	-121.5104W	56812	61
BF09	07,31,76	1543	48.3285N	-121.5097W	56846	95
BF10	07,31,76	1544	48.3289N	-121.5090W	56833	82
BF11	07,31,76	1546	48.3298N	-121.5085W	56853	102
BF12	07,31,76	1547	48.3305N	-121.5083W	56836	85
BF13	07,31,76	1548	48.3312N	-121.5081W	56857	106
BF14	07,31,76	1549	48.3319N	-121.5077W	56867	116
BF15	07,31,76	1551	48.3327N	-121.5074W	56853	102
BF16	07,31,76	1552	48.3333N	-121.5071W	56849	98
BF17	07,31,76	1553	48.3340N	-121.5068W	56883	132
BF18	07,31,76	1554	48.3348N	-121.5067W	56886	135
BG00	07,31,76	1354	48.3504N	-121.5008W	56724	-27
BG01	07,31,76	1355	48.3498N	-121.5015W	56776	25
BG02	07,31,76	1357	48.3495N	-121.5025W	56761	10
BG03	07,31,76	1358	48.3492N	-121.5035W	56848	97
BG04	07,31,76	1359	48.3489N	-121.5047W	56771	20
BG05	07,31,76	1400	48.3484N	-121.5055W	56762	11
BG06	07,31,76	1401	48.3476N	-121.5055W	56790	39
BG07	07,31,76	1402	48.3468N	-121.5051W	56794	43
BG08	07,31,76	1403	48.3460N	-121.5047W	56743	-8
BG09	07,31,76	1405	48.3452N	-121.5044W	56816	65
BG10	07,31,76	1406	48.3444N	-121.5041W	56780	29
BG11	07,31,76	1407	48.3436N	-121.5037W	56812	61
BG12	07,31,76	1409	48.3428N	-121.5034W	56786	35
BG13	07,31,76	1410	48.3420N	-121.5033W	56818	67
BG14	07,31,76	1411	48.3412N	-121.5035W	56807	56
BG15	07,31,76	1412	48.3404N	-121.5037W	56805	54
BG16	07,31,76	1413	48.3396N	-121.5039W	56761	10
BG17	07,31,76	1415	48.3387N	-121.5041W	56760	9
BG18	07,31,76	1416	48.3379N	-121.5044W	56812	61
BG19	07,31,76	1417	48.3370N	-121.5046W	56705	-46
BG20	07,31,76	1418	48.3364N	-121.5050W	56841	90
BG21	07,31,76	1419	48.3357N	-121.5056W	56822	71
BF00	07,31,76	1412	48.3350N	-121.5064W	56873	122
BM00	08,01,76	1507	48.3173N	-121.5253W	56840	89
BM01	08,01,76	1508	48.3172N	-121.5243W	56854	103
BM02	08,01,76	1510	48.3171N	-121.5231W	56846	95
BM03	08,01,76	1511	48.3171N	-121.5218W	56802	51
BM04	08,01,76	1512	48.3171N	-121.5205W	56808	57
BM05	08,01,76	1513	48.3171N	-121.5193W	56810	59
BM06	08,01,76	1514	48.3171N	-121.5183W	56831	80
BM07	08,01,76	1516	48.3170N	-121.5169W	56813	62
BM08	08,01,76	1517	48.3170N	-121.5156W	56807	56
BM09	08,01,76	1518	48.3170N	-121.5145W	56800	49
BM10	08,01,76	1520	48.3170N	-121.5134W	56801	50
BM11	08,01,76	1521	48.3170N	-121.5121W	56773	22
BM12	08,01,76	1522	48.3170N	-121.5107W	56770	19
BM13	08,01,76	1524	48.3170N	-121.5096W	56772	21

BM14	08,01,76	1525	48.3170N	-121.5086W	56753	2
BM15	08,01,76	1527	48.3171N	-121.5074W	56767	12
BM16	08,01,76	1530	48.3172N	-121.5061W	56754	3
BM17	08,01,76	1531	48.3173N	-121.5049W	56726	-25
BM18	08,01,76	1533	48.3174N	-121.5038W	56763	12
BM19	08,01,76	1535	48.3175N	-121.5025W	56751	0
BM20	08,01,76	1537	48.3175N	-121.5012W	56766	15
BM21	08,01,76	1538	48.3175N	-121.5003W	56775	24
BM22	08,01,76	1540	48.3175N	-121.4991W	56765	14
BN00	08,01,76	1541	48.3175N	-121.4985W	56776	25
BP00	08,02,76	1049	48.3442N	-121.5337W	56938	87
BP01	08,02,76	1053	48.3434N	-121.5335W	56863	112
BP02	08,02,76	1054	48.3426N	-121.5335W	56829	78
BP03	08,02,76	1056	48.3418N	-121.5334W	56844	93
BP04	08,02,76	1057	48.3409N	-121.5333W	56835	84
BP05	08,02,76	1059	48.3402N	-121.5332W	56930	79
BP06	08,02,76	1100	48.3394N	-121.5331W	56809	58
BP07	08,02,76	1101	48.3386N	-121.5331W	56827	76
BP08	08,02,76	1102	48.3377N	-121.5331W	56785	34
BP09	08,02,76	1103	48.3369N	-121.5330W	56771	20
BP10	08,02,76	1105	48.3360N	-121.5329W	56787	35
BP11	08,02,76	1106	48.3353N	-121.5329W	56764	13
BT00	08,02,76	1107	48.3346N	-121.5328W	56808	57
BR01	08,02,76	1123	48.3434N	-121.5332W	56790	39
BR02	08,02,76	1125	48.3432N	-121.5321W	56818	67
BR03	08,02,76	1126	48.3431N	-121.5308W	56844	93
BR04	08,02,76	1127	48.3433N	-121.5296W	56828	77
BR05	08,02,76	1129	48.3439N	-121.5286W	56824	73
BR06	08,02,76	1130	48.3443N	-121.5276W	56861	110
BR07	08,02,76	1131	48.3445N	-121.5263W	56876	85
BR08	08,02,76	1132	48.3442N	-121.5251W	56858	107
BR09	08,02,76	1133	48.3437N	-121.5241W	56816	65
BR10	08,02,76	1135	48.3432N	-121.5232W	56810	59
BR11	08,02,76	1136	48.3426N	-121.5222W	56851	100
BR12	08,02,76	1137	48.3423N	-121.5209W	56827	76
BR13	08,02,76	1139	48.3422N	-121.5198W	56816	65
BR14	08,02,76	1140	48.3423N	-121.5185W	56810	59
BR15	08,02,76	1141	48.3426N	-121.5174W	56809	58
BR16	08,02,76	1142	48.3431N	-121.5165W	56797	46
BR00	08,02,76	1143	48.3433N	-121.5157W	56791	40
BB00	08,01,76	1157	48.3242N	-121.5336W	56864	113
BB01	08,01,76	1159	48.3243N	-121.5329W	56883	132
BB02	08,01,76	1200	48.3243N	-121.5321W	56899	147
BB03	08,01,76	1202	48.3244N	-121.5314W	56896	145
BB04	08,01,76	1204	48.3245N	-121.5304W	56865	114
BB05	08,01,76	1205	48.3246N	-121.5297W	56880	129
BB06	08,01,76	1207	48.3246N	-121.5290W	56785	37
BB07	08,01,76	1209	48.3247N	-121.5282W	56848	97
BB08	08,01,76	1210	48.3248N	-121.5275W	56858	107
BB09	08,01,76	1212	48.3253N	-121.5266W	56842	91
BB10	08,01,76	1214	48.3256N	-121.5261W	56824	73
BB11	08,01,76	1215	48.3259N	-121.5254W	56931	180
BB12	08,01,76	1217	48.3262N	-121.5248W	56799	48
BB13	08,01,76	1219	48.3266N	-121.5242W	56863	112
BB14	08,01,76	1221	48.3269N	-121.5236W	56843	92
BB15	08,01,76	1223	48.3273N	-121.5233W	56852	101
BB16	08,01,76	1225	48.3279N	-121.5233W	56817	65
BB17	08,01,76	1226	48.3283N	-121.5236W	56793	42
BB18	08,01,76	1229	48.3287N	-121.5242W	56867	116
BB19	08,01,76	1231	48.3290N	-121.5447W	56849	98
BB20	08,01,76	1232	48.3290N	-121.5254W	56941	93
BB21	08,01,76	1235	48.3291N	-121.5261W	56865	114
BB22	08,01,76	1236	48.3296N	-121.5265W	56844	93
BB23	08,01,76	1238	48.3302N	-121.5264W	56855	104
BB24	08,01,76	1240	48.3303N	-121.5257W	56861	110
BB25	08,01,76	1244	48.3303N	-121.5247W	56832	81
BB26	08,01,76	1247	48.3304N	-121.5241W	56844	93
BB27	08,01,76	1249	48.3307N	-121.5234W	56820	69

8328	08,01,76	1251	48.3306N	-121.5227W	56840	89
8329	08,01,76	1253	48.3303N	-121.5220W	56856	105
8330	08,01,76	1300	48.3300N	-121.5201W	56822	71
8331	08,01,76	1302	48.3298N	-121.5205W	56816	65
8332	08,01,76	1304	48.3295N	-121.5200W	56800	49
8333	08,01,76	1305	48.3293N	-121.5192W	56826	75
8334	08,01,76	1307	48.3293N	-121.5184W	56798	47
8335	08,01,76	1308	48.3293N	-121.5176W	56840	89
8336	08,01,76	1310	48.3294N	-121.5169W	56823	72
8337	08,01,76	1312	48.3296N	-121.5158W	56789	38
8338	08,01,76	1316	48.3297N	-121.5153W	56820	69
8000	08,01,76	1318	48.3299N	-121.5148W	56761	10
8C01	07,31,76	1640	48.3244N	-121.5347W	56874	123
8C02	07,31,76	1641	48.3246N	-121.5356W	56849	98
8C03	07,31,76	1642	48.3246N	-121.5368W	56852	101
8C04	07,31,76	1643	48.3249N	-121.5379W	56849	98
8C05	07,31,76	1644	48.3255N	-121.5386W	56862	111
8C06	07,31,76	1646	48.3260N	-121.5396W	56864	113
8C07	07,31,76	1648	48.3266N	-121.5406W	56790	39
8C08	07,31,76	1649	48.3269N	-121.5411W	56877	126
8C09	07,31,76	1650	48.3279N	-121.5415W	56866	115
8C10	07,31,76	1651	48.3284N	-121.5420W	56887	136
8C11	07,31,76	1652	48.3288N	-121.5429W	56831	80
8C00	07,31,76	1654	48.3292N	-121.5440W	56856	105
8001	08,02,76	1033	48.3440N	-121.5347W	56870	119
8002	08,02,76	1034	48.3441N	-121.5358W	56795	44
8003	08,02,76	1035	48.3443N	-121.5371W	56812	61
8004	08,02,76	1036	48.3444N	-121.5382W	56804	53
8005	08,02,76	1038	48.3445N	-121.5393W	56863	112
8006	08,02,76	1039	48.3447N	-121.5404W	56804	53
8007	08,02,76	1040	48.3449N	-121.5416W	56743	-8
8000	08,02,76	1041	48.3450N	-121.5427W	56788	37
8S01	08,02,76	1207	48.3448N	-121.5330W	56844	93
8S02	08,02,76	1208	48.3456N	-121.5327W	56824	73
8S03	08,02,76	1209	48.3463N	-121.5322W	56865	114
8S04	08,02,76	1211	48.3468N	-121.5315W	56896	145
8S05	08,02,76	1212	48.3476N	-121.5310W	56905	154
8S06	08,02,76	1213	48.3483N	-121.5305W	56918	167
8S07	08,02,76	1214	48.3490N	-121.5301W	56845	94
8S00	08,02,76	1220	48.3498N	-121.5297W	57349	598
8U00	08,02,76	1421	48.3580N	-121.5255W	56756	5
8U01	08,02,76	1424	48.3575N	-121.5261W	56838	87
8U02	08,02,76	1425	48.3568N	-121.5261W	56817	66
8U03	08,02,76	1426	48.3560N	-121.5258W	56773	22
8U04	08,02,76	1427	48.3552N	-121.5264W	56836	85
8U05	08,02,76	1429	48.3548N	-121.5271W	56861	110
8U06	08,02,76	1430	48.3542N	-121.5277W	56810	59
8U07	08,02,76	1413	48.3534N	-121.5282W	56831	80
8U08	08,02,76	1432	48.3527N	-121.5284W	56851	100
8U09	08,02,76	1433	48.3521N	-121.5286W	56852	101
8U10	08,02,76	1435	48.3513N	-121.5288W	56846	95
8U11	08,02,76	1436	48.3507N	-121.5292W	56843	92
8U12	08,02,76	1437	48.3500N	-121.5297W	56851	100
8V01	08,02,76	1338	48.3585N	-121.5243W	56778	27
8V02	08,02,76	1339	48.3587N	-121.5235W	56761	10
8V03	08,02,76	1341	48.3592N	-121.5223W	56740	-11
8V04	08,02,76	1342	48.3595N	-121.5211W	56777	26
8V05	08,02,76	1344	48.3600N	-121.5203W	56793	42
8V06	08,02,76	1345	48.3606N	-121.5194W	56779	28
8V07	08,02,76	1346	48.3612N	-121.5186W	56775	24
8V08	08,02,76	1347	48.3616N	-121.5176W	56756	5
8V09	08,02,76	1349	48.3620N	-121.5267W	56742	-9
8V10	08,02,76	1356	48.3626N	-121.5156W	56753	2
8V11	08,02,76	1357	48.3630N	-121.5146W	56762	11
8V12	08,02,76	1358	48.3633N	-121.5137W	56795	44
8V13	08,02,76	1400	48.3638N	-121.5127W	56801	50
8V14	08,02,76	1401	48.3643N	-121.5116W	56808	57
8V00	08,02,76	1402	48.3646N	-121.5110W	56767	16

BI00	07,31,76	1221	48.3589N	-121.5021W	56805	54
BI01	07,31,76	1223	48.3585N	-121.5020W	56750	-1
BI02	07,31,76	1226	48.3576N	-121.5021W	56817	66
BI03	07,31,76	1228	48.3568N	-121.5020W	56814	63
BI04	07,31,76	1229	48.3559N	-121.5021W	56741	-10
BI05	07,31,76	1231	48.3552N	-121.5021W	56757	6
BI06	07,31,76	1232	48.3545N	-121.5018W	56754	3
BI07	07,31,76	1234	48.3537N	-121.5009W	56762	11
BI08	07,31,76	1235	48.3528N	-121.5007W	56746	-5
BI09	07,31,76	1237	48.3520N	-121.5008W	56757	6
BI10	07,31,76	1238	48.3512N	-121.5007W	56761	10
BH01	07,31,76	1137	48.3597N	-121.5020W	56795	44
BH02	07,31,76	1139	48.3605N	-121.5022W	56824	73
BH03	07,31,76	1141	48.3612N	-121.5020W	56832	81
BH04	07,31,76	1143	48.3620N	-121.5018W	56881	130
BH05	07,31,76	1144	48.3629N	-121.5018W	56828	77
BH06	07,31,76	1146	48.3636N	-121.5020W	56757	6
BH07	07,31,76	1148	48.3645N	-121.5021W	56829	78
BH08	07,31,76	1149	48.3652N	-121.5016W	56855	104
BH09	07,31,76	1150	48.3656N	-121.5005W	56766	15
BH10	07,31,76	1152	48.3660N	-121.4995W	56914	163
BH11	07,31,76	1153	48.3665N	-121.4986W	56771	20
BH12	07,31,76	1155	48.3670N	-121.4976W	56791	40
BH13	07,31,76	1157	48.3673N	-121.4965W	56885	134
BH14	07,31,76	1158	48.3671N	-121.4954W	56879	128
BH15	07,31,76	1160	48.3668N	-121.4943W	56804	53
BH00	07,31,76	1201	48.3665N	-121.4932W	56952	201
BX00	08,02,76	1519	48.3709N	-121.4958W	56732	-19
BX01	08,02,76	1521	48.3710N	-121.4971W	56836	85
BX02	08,02,76	1528	48.3710N	-121.4986W	56735	-16
BX03	08,02,76	1530	48.3707N	-121.5000W	56726	-25
BX04	08,02,76	1531	48.3705N	-121.5016W	56763	12
BX05	08,02,76	1532	48.3703N	-121.5031W	56864	113
BX06	08,02,76	1534	48.3706N	-121.5044W	56773	22
BX07	08,02,76	1535	48.3701N	-121.5057W	56723	-28
BX08	08,02,76	1536	48.3699N	-121.5070W	56771	20
BX09	08,02,76	1537	48.3692N	-121.5081W	56793	42
BX10	08,02,76	1538	48.3684N	-121.5090W	56771	20
BX11	08,02,76	1541	48.3675N	-121.5096W	56755	4
BX12	08,02,76	1543	48.3665N	-121.5101W	56809	58
BX13	08,02,76	1544	48.3655N	-121.5104W	56789	38
AA00	07,29,76	1156	48.3252N	-121.4335W	56653	-98
AG01	07,29,76	1202	48.3245N	-121.4342W	56798	47
AG02	07,29,76	1205	48.3247N	-121.4356W	56721	-30
AG03	07,29,76	1208	48.3252N	-121.4367W	56661	-90
AG00	07,29,76	1215	48.3251N	-121.4380W	56784	33
AA01	07,29,76	1222	48.3244N	-121.4336W	56827	76
AA02	07,29,76	1224	48.3236N	-121.4335W	56819	68
AA03	07,29,76	1226	48.3228N	-121.4332W	56836	85
AA04	07,29,76	1227	48.3221N	-121.4330W	56789	38
AA05	07,29,76	1228	48.3213N	-121.4326W	56639	-112
AA06	07,29,76	1230	48.3204N	-121.4326W	56798	47
AA07	07,29,76	1231	48.3197N	-121.4320W	56799	48
AA08	07,29,76	1232	48.3190N	-121.4316W	56745	-6
AA09	07,29,76	1234	48.3182N	-121.4310W	56748	-3
AA10	07,29,76	1235	48.3175N	-121.4306W	56783	32
AA11	07,29,76	1236	48.3168N	-121.4301W	56770	19
AA12	07,29,76	1239	48.3161N	-121.4236W	56772	21
AA13	07,29,76	1241	48.3153N	-121.4291W	56795	44
AA14	07,29,76	1242	48.3146N	-121.4286W	56782	31
AA15	07,29,76	1243	48.3139N	-121.4279W	56652	-99
AA16	07,29,76	1244	48.3132N	-121.4270W	56754	3
AA17	07,29,76	1246	48.3126N	-121.4263W	56767	16
AA18	07,29,76	1247	48.3121N	-121.4255W	56789	38
AA19	07,29,76	1249	48.3115N	-121.4248W	56596	-155
AA20	07,29,76	1252	48.3108N	-121.4242W	56777	26
AA21	07,29,76	1253	48.3101N	-121.4237W	56786	35
AA22	07,29,76	1254	48.3094N	-121.4230W	56770	19

AA23	07,29,76	1256	48.3087N	-121.4221W	56790	39
AA24	07,29,76	1257	48.3082N	-121.4212W	56774	23
AA25	07,29,76	1258	48.3075N	-121.4208W	56754	3
AA26	07,29,76	1300	48.3067N	-121.4202W	56701	-50
AA27	07,29,76	1302	48.3059N	-121.4197W	56697	-54
AA28	07,29,76	1303	48.3053N	-121.4191W	56712	-39
AA29	07,29,76	1304	48.3045N	-121.4187W	56687	-64
AA30	07,29,76	1306	48.3038N	-121.4183W	56799	48
AF00	07,29,76	1307	48.3032N	-121.4175W	56645	-106
AB01	07,29,76	1442	48.3260N	-121.4339W	56673	-78
AB02	07,29,76	1443	48.3267N	-121.4339W	56870	119
AB03	07,29,76	1445	48.3274N	-121.4341W	56785	34
AB04	07,29,76	1446	48.3281N	-121.4342W	56732	-19
AB05	07,29,76	1447	48.3287N	-121.4341W	56748	-3
AB06	07,29,76	1448	48.3295N	-121.4339W	56730	-21
AB07	07,29,76	1450	48.3303N	-121.4338W	56758	7
AB08	07,29,76	1451	48.3310N	-121.4338W	56736	-15
AB09	07,29,76	1452	48.3317N	-121.4337W	56759	8
AB10	07,29,76	1454	48.3324N	-121.4335W	56759	8
AB11	07,29,76	1455	48.3332N	-121.4331W	56745	-6
AB12	07,29,76	1456	48.3338N	-121.4330W	56758	7
AB13	07,29,76	1458	48.3347N	-121.4326W	56753	2
AB14	07,29,76	1459	48.3353N	-121.4322W	56762	11
AB15	07,29,76	1503	48.3358N	-121.4316W	56760	9
AB00	07,29,76	1502	48.3355N	-121.4307W	56751	0
AD01	07,29,76	1553	48.3200N	-121.4196W	56753	2
AD02	07,29,76	1555	48.3209N	-121.4198W	56755	4
AD03	07,29,76	1557	48.3217N	-121.4198W	56758	7
AD04	07,29,76	1558	48.3224N	-121.4196W	56759	8
AD05	07,29,76	1559	48.3232N	-121.4193W	56757	6
AD06	07,29,76	1600	48.3240N	-121.4195W	56743	-8
AD07	07,29,76	1602	48.3248N	-121.4198W	56756	5
AD08	07,29,76	1603	48.3255N	-121.4202W	56757	6
AD09	07,29,76	1604	48.3263N	-121.4203W	56764	13
AD10	07,29,76	1606	48.3271N	-121.4203W	56770	19
AD11	07,29,76	1608	48.3278N	-121.4201W	56758	7
AD12	07,29,76	1609	48.3286N	-121.4200W	56758	7
AD13	07,29,76	1610	48.3294N	-121.4196W	56752	1
AD14	07,29,76	1611	48.3302N	-121.4196W	56759	8
AD15	07,29,76	1613	48.3311N	-121.4195W	56651	-100
AD16	07,29,76	1614	48.3318N	-121.4193W	56755	4
AD17	07,29,76	1616	48.3323N	-121.4185W	56758	7
AD18	07,29,76	1618	48.3323N	-121.4171W	56755	4
AD19	07,29,76	1620	48.3324N	-121.4164W	56759	8
AD20	07,29,76	1621	48.3326N	-121.4151W	56758	7
AD00	07,29,76	1623	48.3331N	-121.4142W	56759	8
AC00	07,30,76	1204	48.3192N	-121.4196W	56629	-122
AC01	07,30,76	1206	48.3194N	-121.4206W	56771	20
AC02	07,30,76	1207	48.3201N	-121.4212W	56704	-47
AC03	07,30,76	1209	48.3206N	-121.4220W	56778	27
AC04	07,30,76	1210	48.3213N	-121.4226W	56777	26
AC05	07,30,76	1211	48.3220N	-121.4232W	56769	18
AC06	07,30,76	1212	48.3226N	-121.4237W	56766	15
AC07	07,30,76	1213	48.3232N	-121.4244W	56775	24
AC08	07,30,76	1214	48.3239N	-121.4250W	56768	17
AC09	07,30,76	1216	48.3246N	-121.4255W	56770	19
AC10	07,30,76	1217	48.3254N	-121.4259W	56782	31
AC11	07,30,76	1218	48.3262N	-121.4261W	56778	27
AC12	07,30,76	1219	48.3269N	-121.4263W	56783	32
AC13	07,30,76	1220	48.3275N	-121.4268W	56771	20
AC14	07,30,76	1222	48.3283N	-121.4272W	56777	26
AC15	07,30,76	1223	48.3290N	-121.4277W	56786	35
AC16	07,30,76	1237	48.3297N	-121.4281W	56785	34
AC17	07,30,76	1238	48.3304N	-121.4285W	56787	36
AC18	07,30,76	1239	48.3313N	-121.4288W	56782	31
AC19	07,30,76	1241	48.3319N	-121.4291W	56764	13
AC20	07,30,76	1242	48.3326N	-121.4295W	56775	24
AC21	07,30,76	1243	48.3333N	-121.4300W	56802	51

AC22	07,30,76	1244	48.3341N	-121.4306W	56771	20
AC23	07,30,76	1245	48.3348N	-121.4307W	56774	23
AE01	07,30,76	1321	48.3190N	-121.4185W	56681	-70
AE02	07,30,76	1323	48.3187N	-121.4171W	56766	15
AE03	07,30,76	1325	48.3182N	-121.4163W	56755	4
AE04	07,30,76	1326	48.3172N	-121.4157W	56750	-1
AE05	07,30,76	1328	48.3162N	-121.4152W	56752	1
AE06	07,30,76	1330	48.3159N	-121.4149W	56745	-5
AE00	07,30,76	1331	48.3154N	-121.4145W	56822	71
AP01	08,03,76	1126	48.3511N	-121.4207W	56795	44
AP02	08,03,76	1127	48.3503N	-121.4210W	56813	62
AP03	08,03,76	1129	48.3496N	-121.4213W	56808	57
AP04	08,03,76	1130	48.3491N	-121.4221W	56808	57
AP05	08,03,76	1131	48.3485N	-121.4229W	56817	65
AP06	08,03,76	1132	48.3478N	-121.4235W	56818	67
AP07	08,03,76	1134	48.3473N	-121.4245W	56823	72
AP08	08,03,76	1135	48.3474N	-121.4256W	56815	64
AP09	08,03,76	1137	48.3473N	-121.4266W	56835	84
AP10	08,03,76	1138	48.3469N	-121.4276W	56818	67
AP11	08,03,76	1139	48.3464N	-121.4283W	56826	75
AP12	08,03,76	1140	48.3456N	-121.4289W	56830	79
AP13	08,03,76	1141	48.3448N	-121.4292W	56830	79
AP14	08,03,76	1143	48.3442N	-121.4295W	56830	79
A000	08,03,76	1144	48.3436N	-121.4298W	56839	88
AS00	08,03,76	1310	48.3581N	-121.4245W	56846	95
AS01	08,03,76	1311	48.3574N	-121.4244W	56829	78
AS02	08,03,76	1313	48.3567N	-121.4245W	56826	75
AS03	08,03,76	1314	48.3560N	-121.4245W	56832	81
AS04	08,03,76	1315	48.3553N	-121.4239W	56820	69
AS05	08,03,76	1316	48.3551N	-121.4229W	56824	73
AS06	08,03,76	1317	48.3550N	-121.4218W	56822	71
AS07	08,03,76	1318	48.3547N	-121.4209W	56828	77
AS08	08,03,76	1320	48.3548N	-121.4199W	56818	67
AS09	08,03,76	1321	48.3551N	-121.4188W	56774	23
AS10	08,03,76	1323	48.3554N	-121.4177W	56791	40
AS11	08,03,76	1325	48.3556N	-121.4168W	56794	43
AS12	08,03,76	1326	48.3558N	-121.4157W	56784	33
AS13	08,03,76	1327	48.3559N	-121.4147W	56810	59
AS14	08,03,76	1328	48.3560N	-121.4136W	56814	63
AS15	08,03,76	1329	48.3561N	-121.4125W	56793	42
AS16	08,03,76	1330	48.3561N	-121.4114W	56810	59
AT01	08,03,76	1350	48.3587N	-121.4250W	56830	79
AT02	08,03,76	1351	48.3596N	-121.4251W	56832	81
AT03	08,03,76	1353	48.3602N	-121.4256W	56815	64
AT04	08,03,76	1354	48.3608N	-121.4267W	56769	18
AT05	08,03,76	1356	48.3602N	-121.4267W	57440	689
AT06	08,03,76	1358	48.3595N	-121.4268W	56807	56
AT07	08,03,76	1400	48.3587N	-121.4269W	56807	56
AT08	08,03,76	1401	48.3580N	-121.4271W	56804	53
AT09	08,03,76	1402	48.3572N	-121.4273W	56797	46
AT10	08,03,76	1404	48.3566N	-121.4279W	56794	43
AT11	08,03,76	1405	48.3559N	-121.4286W	56791	40
AT12	08,03,76	1406	48.3553N	-121.4293W	56783	32
AT13	08,03,76	1407	48.3548N	-121.4300W	56754	3
AT14	08,03,76	1408	48.3541N	-121.4305W	56866	115
AT15	08.03,76	1410	48.3534N	-121.4307W	56850	99
AT00	08,03,76	1411	48.3528N	-121.4310W	56871	120
AT16	08,03,76	1412	48.3531N	-121.4319W	56836	85
AR01	08,03,76	1457	48.3442N	-121.4307W	56818	67
AR02	08,03,76	1458	48.3447N	-121.4316W	56827	76
AR03	08,03,76	1459	48.3451N	-121.4326W	56983	232
AR04	08,03,76	1501	48.3456N	-121.4333W	56813	62
AR05	08,03,76	1502	48.3462N	-121.4343W	56820	69
AR06	08,03,76	1503	48.3467N	-121.4350W	56893	142
AR07	08,03,76	1505	48.3472N	-121.4357W	56831	80
AR08	08,03,76	1506	48.3477N	-121.4365W	56816	65
AR09	08,03,76	1507	48.3482N	-121.4373W	56810	59
AR10	08.03,76	1509	48.3486N	-121.4385W	56799	48

AR11	08,03,76	1510	48.3490N	-121.4396W	56807	56
AR12	08,03,76	1511	48.3494N	-121.4406W	56800	49
AR13	08,03,76	1512	48.3498N	-121.4413W	56801	50
AR14	08,03,76	1513	48.3502N	-121.4428W	56784	33
AR00	08,03,76	1514	48.3507N	-121.4434W	56772	21
AP00	08,03,76	1050	48.3518N	-121.4209W	56806	55
AO01	08,03,76	1053	48.3524N	-121.4215W	56802	51
AO03	08,03,76	1055	48.3529N	-121.4206W	56793	42
AO04	08,03,76	1056	48.3527N	-121.4193W	56786	35
AO05	08,03,76	1058	48.3522N	-121.4183W	56798	47
AO06	08,03,76	1059	48.3528N	-121.4171W	56804	53
AO07	08,03,76	1100	48.3535N	-121.4164W	56800	49
AO08	08,03,76	1102	48.3540N	-121.4157W	56802	51
AO09	08,03,76	1103	48.3546N	-121.4149W	56751	-59
AO10	08,03,76	1104	48.3551N	-121.4139W	56799	43
AO11	08,03,76	1106	48.3553N	-121.4129W	56816	65
AO12	08,03,76	1107	48.3557N	-121.4118W	56816	65
AO00	08,03,76	1109	48.3562N	-121.4109W	56807	56
AF01	07,30,76	1452	48.3028N	-121.4079W	56727	-24
AF02	07,30,76	1453	48.3025N	-121.4071W	56712	-39
AF03	07,30,76	1455	48.3019N	-121.4064W	56774	23
AF04	07,30,76	1456	48.3013N	-121.4058W	56734	-17
AF05	07,30,76	1459	48.3009N	-121.4050W	56744	-7
AF06	07,30,76	1501	48.3004N	-121.4042W	56738	-13
AF07	07,30,76	1502	48.2998N	-121.4037W	56721	-30
AF08	07,30,76	1504	48.2991N	-121.4033W	56716	-35
AF09	07,30,76	1505	48.2984N	-121.4029W	56708	-43
AF10	07,30,76	1507	48.2978N	-121.4025W	56753	2
AF11	07,30,76	1509	48.2972N	-121.4021W	56720	-31
AF12	07,30,76	1510	48.2968N	-121.4012W	56720	-31
AF13	07,30,76	1512	48.2964N	-121.4002W	56673	-78
AF14	07,30,76	1514	48.2961N	-121.3993W	56696	-55
AJ00	07,30,76	1515	48.2953N	-121.3988W	56644	-107
AL00	07,30,76	1610	48.2635N	-121.3934W	56713	-38
AM01	07,30,76	1614	48.2635N	-121.3947W	56727	-24
AM02	07,30,76	1617	48.2635N	-121.3959W	56729	-22
AM03	07,30,76	1619	48.2640N	-121.3969W	56729	-22
AM04	07,30,76	1621	48.2646N	-121.3977W	56716	-33
AM05	07,30,76	1623	48.2652N	-121.3985W	56714	-37
AM06	07,30,76	1624	48.2660N	-121.3992W	56709	-42
AM07	07,30,76	1626	48.2667N	-121.3996W	56748	-3
AM00	07,30,76	1625	48.2676N	-121.4001W	56739	-12
AN01	07,30,76	1645	48.2637N	-121.3924W	56720	-31
AN02	07,30,76	1647	48.2638N	-121.3914W	56717	-34
AN03	07,30,76	1649	48.2639N	-121.3905W	56719	-32
AN04	07,30,76	1651	48.2640N	-121.3894W	56726	-25
AN05	07,30,76	1653	48.2641N	-121.3883W	56725	-26
AN06	07,30,76	1654	48.2642N	-121.3873W	56731	-23
AN07	07,30,76	1657	48.2643N	-121.3863W	56695	-56
AN08	07,30,76	1658	48.2644N	-121.3852W	56752	1
AN00	07,30,76	1660	48.2644N	-121.3842W	56786	35

APPENDIX C

APPENDIX C

Nooksack Sandstones

The samples used in this study were collected along the Glacier Creek road in T39N, R7E. Sample 76-RL-30 (a and b) was collected in a road cut in the SW1/4 of section 9. Sample 76-RL-29 was collected in a road cut in the SE1/4 of section 16. The outcrops visited had rhythmic, graded beds. The beds were steeply dipping with a few sandstone beds interbedded with many siltstone beds. The textures noticed in thin section were poor to moderate sorting and angular to rounded grains. The sandstones studied were texturally and compositionally immature. The rocks are of Early Cretaceous age (Misch, 1966).

Chilliwack Sandstone from Jackman Creek

Outcrops of Chilliwack sandstones are found in road cuts along Jackman Creek. The samples used in this study were collected in the SW1/4 of section 12, T35N, R8E, and the NW1/4 of section 4, T35N, R9E. Textures seen in thin section were poor to moderate sorting and angular to subangular grains. The sandstones studied were texturally and compositionally immature. Limestones near the collecting localities contain Devonian fossils (Danner, 1966).

Appendix Table C-1. Modal analysis of four chilliwack sandstones from the thesis area.

	Volume Percent				Adjusted Volume Percent	
Mineralogy	JAD-76-111	JAD-76-122	JAD-76-122	JAD-76-188	JAD-76-122	JAD-76-188
quartz	13.8%	15.8%	29.2%	16.8%	46%	36%
polycrystalline quartz	23.0	5.4	----	4.9	----	11
plagioclase	4.4	t	6.9	3.5	12	8
orthoclase	8.0	1.0	6.1	5.6	10	12
opaques	t	----	1.2	2.3	2	5
muscovite	t	----	t	t	----	----
hornblende	t	----	t	t	----	----
clinopyroxene	t	----	----	----	----	----
olivine	t	----	----	----	----	----
volcanic lithics	25.7	62.8	19.2	3.7	30	8
chert	1.8	----	----	8.5	----	18
granitics	t	1.0	----	----	----	----
phylite	t	----	----	----	----	----
schist	1.4	----	----	----	----	----
matrix	19.3	14.0	36.7	46.2		
vein quartz	----	----	----	7.3		
TOTAL	97.4	100.0	99.3	98.8	100	98
Points counted	725	530	600	700		
Grain Size	medium	very coarse	fine	fine	fine	fine

t = trace, --- = 0.0%

Appendix Table C-2. Modal analysis of three chilliwack sandstones from Jackman Creek.

Mineralogy	76-RL-23a	76-RL-25a	76-RL-26b
quartz	7.2%	6.5%	11.6%
polycrystalline quartz	t	----	----
plagioclase	15.8	10.9	9.8
orthoclase	6.3	3.5	8.0
sphene	1.0	----	----
olivine	----	t	----
augite	----	t	----
garnet	----	t	----
opaque	----	t	----
volcanic lithics	43.0	46.4	42.6
sandstone	----	----	t
sandy siltstone	----	t	t
matrix	25.6	31.2	16.9
calcite	t	t	10.6
Total	98.9	98.5	99.5
Points counted	500	550	550
Grain Size	medium	coarse	coarse

t = trace, --- = 0.0%

Appendix Table C-3. Modal analysis of four swauk sandstones.

	Volume Percent			
Mineralogy	JAD-76-48	JAD-76-62	JAD-76-67	JAD-76-206
quartz	22.5%	26.5%	26.0%	21.8%
polycrystalline quartz	5.7	6.7	5.0	6.9
plagioclase	15.5	11.0	14.0	21.8
orthoclase	14.1	10.5	15.0	10.8
perthite	----	----	2.0	----
opaques	----	7.2	t	----
epidote	----	t	----	----
muscovite	t	t	t	t
biotite	6.3	3.0	----	1.8
phlogopite	----	----	2.0	----
hornblende	----	----	t	4.7
clinopyroxene	----	----	1.0	----
orthopyroxene	----	----	----	t
kyanite	t	----	----	----
sphene	----	----	t	t
zircon	----	t	----	----
garnet	----	----	t	----
carbonaceous matter	2.7	----	----	t
volcanic lithics	3.5	4.0	6.0	2.9
granitics	4.9	3.4	4.0	7.9
schist	4.1	2.0	1.0	1.2
phylite	----	----	4.0	----
gneiss	----	----	2.0	3.5
silty mudstone	2.9	----	----	1.4
matrix	17.8	23.3	12.0	14.3
calcite	----	1.5	4.0	----
Total	100.0	99.0	98.0	99.0
Points Counted	511	525	503	509
Grain Size	very coarse	medium	coarse	medium

t = trace, --- = 0.0%

Appendix Table C-4. Modal analysis of three nooksack sandstones from Mt. Baker Quad.

Mineralogy	Volume Percent		
	76-RL-29	76-RL-30a	76-RL-30b
quartz	15.6%	14.8%	15.7%
polycrystalline quartz	1.6	1.4	1.1
plagioclase	19.4	8.5	11.9
orthoclase	13.6	8.0	15.1
apatite	t	----	----
opaques	t	----	----
zircon	----	t	----
volcanic lithics	12.4	21.2	22.3
siltstone	----	21.6	4.9
matrix	37.4	24.7	22.3
calcite	----	----	3.4
radiolarian test	----	----	t
Total	100	100.2	96.7
Points Counted	500	500	530
Grain Size	fine	medium	medium

t = trace, --- = 0.0%

Appendix Table C-5. Modal analysis of the Skagit gneiss and the Hornblende diorite.

Minerals	Skagit gneiss	Hornblende diorite
Quartz	41%	--
Albite	10	--
Andesine	--	14
Actinolite	37	--
Hornblende	--	84
Biotite	9	--
Muscovite	--	t
Garnet	1	t
Magnetite	2	--
Pyrite	--	1
	—	—
TOTAL	100	99
Points Counted	350	300

t = trace, -- = 0.0%